Physica A 555 (2020) 124571

Contents lists available at ScienceDirect

Physica A

journal homepage: www.elsevier.com/locate/physa

Comparison of escalator strategies in models using a modified totally asymmetric simple exclusion process

Hiroki Yamamoto [a,*], Daichi Yanagisawa [b,c], Katsuhiro Nishinari [b,c]

[a] School of Medicine, Hirosaki University, 5 Zaifu-cho Hirosaki city, Aomori, 036-8562, Japan
[b] Research Center for Advanced Science and Technology, The University of Tokyo, 4-6-1 Komaba, Meguro-ku, Tokyo 153-8904, Japan
[c] Department of Aeronautics and Astronautics, School of Engineering, The University of Tokyo, 7-3-1 Hongo, Bunkyo-ku, Tokyo 113-8656, Japan

ARTICLE INFO

Article history:
Received 7 November 2019
Received in revised form 27 March 2020
Available online 17 April 2020

ABSTRACT

We develop a modified version of the totally asymmetric simple exclusion process (TASEP) and use it to reproduce flow on an escalator with two distinct lanes of pedestrian traffic. The model is used to compare strategies with two standing lanes and a standing lane with a walking lane, using theoretical analyses and numerical simulations for the transport of finite number of particles. The results show that two standing lanes are better for smoother overall transportation, while a mixture of standing and walking is advantageous only in limited cases that have a small number of pedestrians. In contrast, with many pedestrians, the individual travel time of the first several entering walking-preference particles is always shorter with distinct standing and walking lanes than it is with two standing lanes.

1. Introduction

An escalator is an essential system for pedestrian transportation in many public facilities, such as train stations, shopping malls, and airports, that enable people to efficiently move. The capacity of an escalator has been investigated throughly [1,2]. Such studies mainly focus on the maximum capacity of the system.

When considering the operation of an escalator after it is installed, individual pedestrian behaviors must also be understood. In many countries, for example, etiquette dictates that people should stand on one side and walk on the other side of an escalator [3–7]. Somewhat counter-intuitively, however, some practitioners have recently started to encourage people to stand on both sides for smoother transportation and safety [8–10].

Research about escalators in the fields of transportation engineering and nonequilibrium statistical mechanics has only recently begun [11–17] . Individual behavior has also been considered. Refs. [11–13] investigate the flow of traffic mainly from numerical simulations, while Refs. [14,15] study pedestrian choices between escalators and stairways. Especially, in Refs. [16,17], they investigate the escalator etiquette (standing on one side and walking on the other side) and conclude that walking is not beneficial in some cases. However, their results are basically obtained using only numerical simulations with some specific parameters. We consider it to be essential to anew investigate which escalator strategy is suitable for various situations using numerical simulations with extensive parameters and theoretical analyses.

* Corresponding author.
E-mail address: h18m1140@hirosaki-u.ac.jp (H. Yamamoto).

https://doi.org/10.1016/j.physa.2020.124571
0378-4371/

Fig. 1. Schematic illustration of the modified escalator model (one lane). The updating rules are summarized in Table 1 (bulk), 2 (right boundary), and 3 (left boundary).

In the present study, we analyze a novel escalator model that reproduces individual pedestrians' behaviors on both macro- (total transportation time or flow) and micro-scales (individual transportation time). Theoretical analyses and numerical simulations are used. To present an escalator, we construct a two-lane model with a modified totally asymmetric simple exclusion process (TASEP), which is a stochastic process on a one-dimensional lattice in which particles are allowed to hop in one direction (left to right in the present study). In the field of nonequilibrium statistical mechanics, researchers have applied TASEP extensively to various themes such as molecular-motor traffic [18–21], vehicular traffic [22–25], and exclusive queuing processes [26–28], and the process is especially useful since it can be solved exactly [29–31]. Our model differs from the original TASEP with open boundaries in two respects.

First, the updating rules for particles are different. Specifically, in addition to the original hopping probability, particles can hop one site as a whole, which is an important feature of an escalator.

Second, our model consists of two lanes that can have different hopping probabilities. Particles have their preference (walking or standing) and select the lane to enter in one strategy. The multi-lane TASEP has itself been investigated vigorously [32–35]; however, most of them assume the same hopping probability in all lanes. Fundamental behaviors of this model like the phase transitions are investigated in Refs. [32,33]. Meanwhile, Refs. [34,35] analyze actual traffic flows using the multi-lane TASEP.

In the present study, we investigate three escalator strategies; (i) Strategy SS: two standing lanes, (ii) Strategy SW: one standing lane with one walking lane, and (iii) Strategy WW: two walking lanes. We note that Strategy SS and SW are our focus, because they are more common.

We conduct theoretical analyses and numerical simulations for the transport of finite number of particles with this model. As a result, we find that Strategy SS is generally more advantageous in terms of reducing the total (macro-scale) transportation time, especially with a relatively large number of particles, which model pedestrians. Conversely, in terms of reducing the individual (micro-scale) transportation time, Strategy SW offers better results for the first-entering particles, which tend to prefer walking, on the escalator.

The rest of this paper is organized as follows. Section 2 defines the modified two-lane TASEP. Then Section 3 discusses the behavior of the basic one-lane model with our modified updating rules. In Section 4, we examine the total transportation time for finite number of particles given with our modified two-lane model. Then, we proceed to discussion of individual transportation times in Section 5. Finally, Section 6 gives concluding remarks.

2. Model description

Our escalator model is constructed modifying the TASEP with open-boundary conditions. Similarly as the original TASEP, the lattice is consisted of L sites, which are labeled from left to right as $i = 0, 1, \ldots, L-1$, as illustrated in Fig. 1. Each site can be either empty or occupied by only one particle (pedestrian). When the ith site at time t is occupied by a particle, its state is represented as $s_i(t) = 1$; otherwise, its state is $s_i(t) = 0$. In the present study discrete time and parallel updating are adopted. During parallel updating, the states of all the particles on the lattice are determined simultaneously in the next time step.

In the bulk particles are updated by the two-step structure. Here, we divide one-time step into two parts for convenience: (1) between time t and $t + 1/2$ and (2) between time $t + 1/2$ and $t + 1$. Between time t and $t + 1/2$, particles hop one site as a whole, which reproduces the escalator automatic movement. Then, between time $t + 1/2$ and $t + 1$ particles hop one more site forward with hopping probability p, which is fixed throughout each lattice in our model, if the right-neighboring site is empty. This possibility represents walking on an escalator. So, particles in the bulk can hop one or two sites for each time step. Table 1 summarizes the updating rules in the bulk of our model from time t and $t + 1$. Due to the updating rules, at the right boundary a particle can leave the system from the $(L-1)$th site or from the $(L-2)$th site. We note that a particle occupying the $(L-1)$th site at time t must leave the system at time $t + 1$. Table 2 extracts and summarizes the updating rules around the right boundary.

In addition, our model consists of two lanes. The state of the ith site of the lane 1 and 2 at time t are represented as $s_i^1(t)$ and $s_i^2(t)$, respectively. Each lane can act as a standing lane ($p = 0$) or a walking lane ($0 < p \leq 1$). Changing lanes is prohibited. Now, we consider three strategies: (1) two standing lanes, corresponding to Strategy SS (see Fig. 2(a)), (2) one standing lane with one walking lane, corresponding to Strategy SW (see Fig. 2(b)), and (3) two walking lanes,

Table 1
Updating rules for the red particles in the bulk of our model from time t and $t+1$. This figure describes three consecutive sites among the $0, 1, \ldots, (L-3)$th sites. The site represented by '*' can be either empty or occupied (those sites do not influence the red particles). We note that the dotted blue circle indicates that the blue particle either remains at the third site or move to the right-neighboring site of the third site, which is not described in this figure, dependent on the state of the right-neighboring site of the third site.

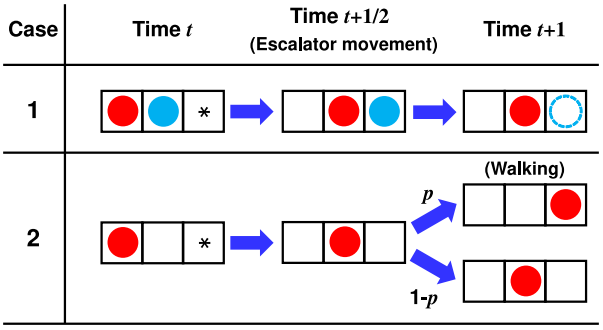

Table 2
Updating rules for the red (blue) particles at the $(L-2)$th ($(L-1)$th) site from time t and $t+1$.

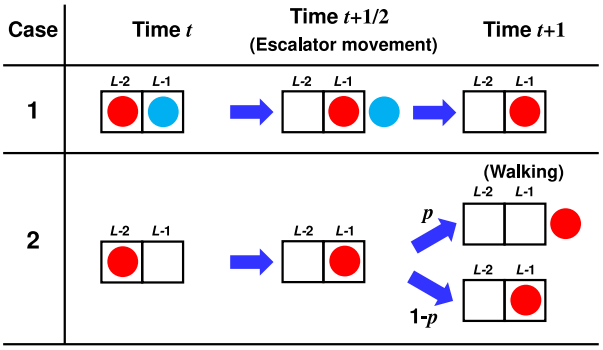

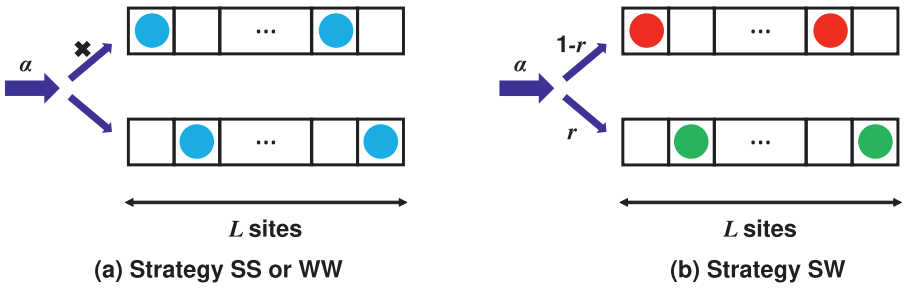

Fig. 2. Schematic illustration of the modified TASEP with (a) Strategy SS (or WW): two standing (walking) lanes, (b) Strategy SW: one standing lane (upper) and one walking lane (lower), and (c) Strategy WW: two walking lanes. We note that the red (green) particles prefer standing (walking) and the blue particles represent indifferently standing- or walking-preference ones.

corresponding to Strategy WW (see Fig. 2(a)). Strategy WW is generally not adopted in real situations; however, it is investigated here for the sake of comparison. We set the input probability to α.

At the left boundary a particle enters the targeted lane with the same rule as the original TASEP. At every time step, at most one particle can enter the system. With Strategy SS and WW, a particle can enter either of the two lanes if the 0th site is empty. Specifically, a particle enters lane 1 and lane 2 if $(s_i^1(t), s_i^2(t)) = (0, 1)$ and if $(s_i^1(t), s_i^2(t)) = (1, 0)$, respectively, while it must select to enter either of two lanes if $(s_i^1(t), s_i^2(t)) = (0, 0)$ indiscriminately, i.e., with probability 1/2. We note that a particle can always enter the system with Strategy SS and WW. This is because all the particles in the bulk will hop one or two sites forward every time step, so at least one of the two left boundaries will always be vacant; that is,

Table 3
Updating rules for the entering blue particle at the left boundary from time t and $t+1$. We note that it can represent indifferently a standing- or walking-preference particle.

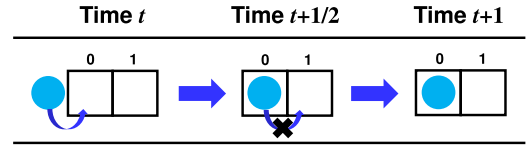

$(s_1^1(t), s_1^2(t)) = (0, 1)$, $(1, 0)$, or $(0, 0)$. With Strategy SW, however, two types of particles are possible; walking-preference particles with probability r and standing-preference particles with probability $1 - r$. Standing- (walking-preference) particles can enter the standing (walking) lane if the leftmost site of the corresponding lane is empty; otherwise they cannot. Unlike Strategy SS and WW, a particle frequently cannot enter the system in this case because of the preference. [1] Table 3 extracts and summarizes the updating rules at the left boundary, featuring only the particle which can enter the system. We note that the entering particle cannot move between time $t + 1/2$ and $t + 1$, i.e., it can only move to the 0th site (cannot move to the 1st site) in one time step.

We describe the pseudo flow diagram for our model with Strategy SW in Fig. 3. This figure will help understand the algorithm of the modified TASEP model.

3. One-lane model with the modified updating rules

In this section, we briefly discuss the steady-state flow of the basic one-lane model (see Fig. 1) with the modified updating rules. We here set the input probability α for one lane.

In this system, particles must hop one or two sites forward. Therefore, the steady-state flow is clearly equal to or more than that of the original TASEP with hopping probability $p = 1$.

The original parallel-updated TASEP with $p = 1$ for various (α, β) exhibits only two phases; the low-density (LD) phase, in which the system is governed by the left boundary, and the high-density (HD) phase, in which the system is governed by the right boundary, and the maximal current (MC) phase, in which the system is governed by the bulk, never occurs. Therefore, the one-lane model is always governed by the left boundary, since a queue can never form near the right boundary. This fact, counter-intuitively, shows that the flow is determined regardless of p, so the flow is always constant. This can be explained as follows.

First, walking clearly reduces the dwell time of each particle in the system, which is defined as the time gap between the time when the particle enters the system and the time when it leaves. The dwell time decreases as p increases. In addition, the global density of the lane, which is defined as the average number of occupied cells over the space $[0, L-1]$ in one time step, decreases as p increases, due to the longer gap between particles. Fig. 4 shows the average dwell time and the global density as functions of p, and reproduce the behavior discussed above. Since (i) the average velocity of particles is proportional to the inverse of the dwell time, and (ii) the flow is represented as a multiplication of the average velocity and the global density, the flow can remain constant.

The steady-state flow Q_1 of the one-lane model with our updating rules satisfies

$$Q_1 = \alpha(1 - Q_1), \tag{1}$$

resulting in

$$Q_1 = \frac{\alpha}{1+\alpha}. \tag{2}$$

Eq. (2) is equal to that of the original TASEP in the LD phase with parallel updating, indicating that the one-lane system always exhibits the LD phase.

Fig. 5 compares the simulation (dots) and theoretical (curve) values of Q as functions of α for various $p \in \{0, 0.5, 1\}$. In the simulations, we set $L = 200$ and the flow is obtained by averaging over 10^5 time steps after evolving the system for 10^4 time steps (and similarly hereafter). In Fig. 5, the simulation values show very good agreement with the theoretical curve, and at the same time, the simulations also confirm that Q_1 is independent on p.

4. Total (macro-scale) transportation time with the two-lane model

In this section, we investigate the total (macro-scale) transportation time T of finite number (N) of particles with the two-lane model. Specifically, T is defined as the time gap between the start of the simulation and the time at which the final leaving particle leaves the system. The total transportation times with Strategy SS, SW, and WW are represented as T_{SS}, T_{SW}, and T_{WW}, respectively.

[1] In the simulations below the preference of a particle is determined just before it enters the system; this preference is reset if the particle cannot enter and is redetermined at the next chance of entering.

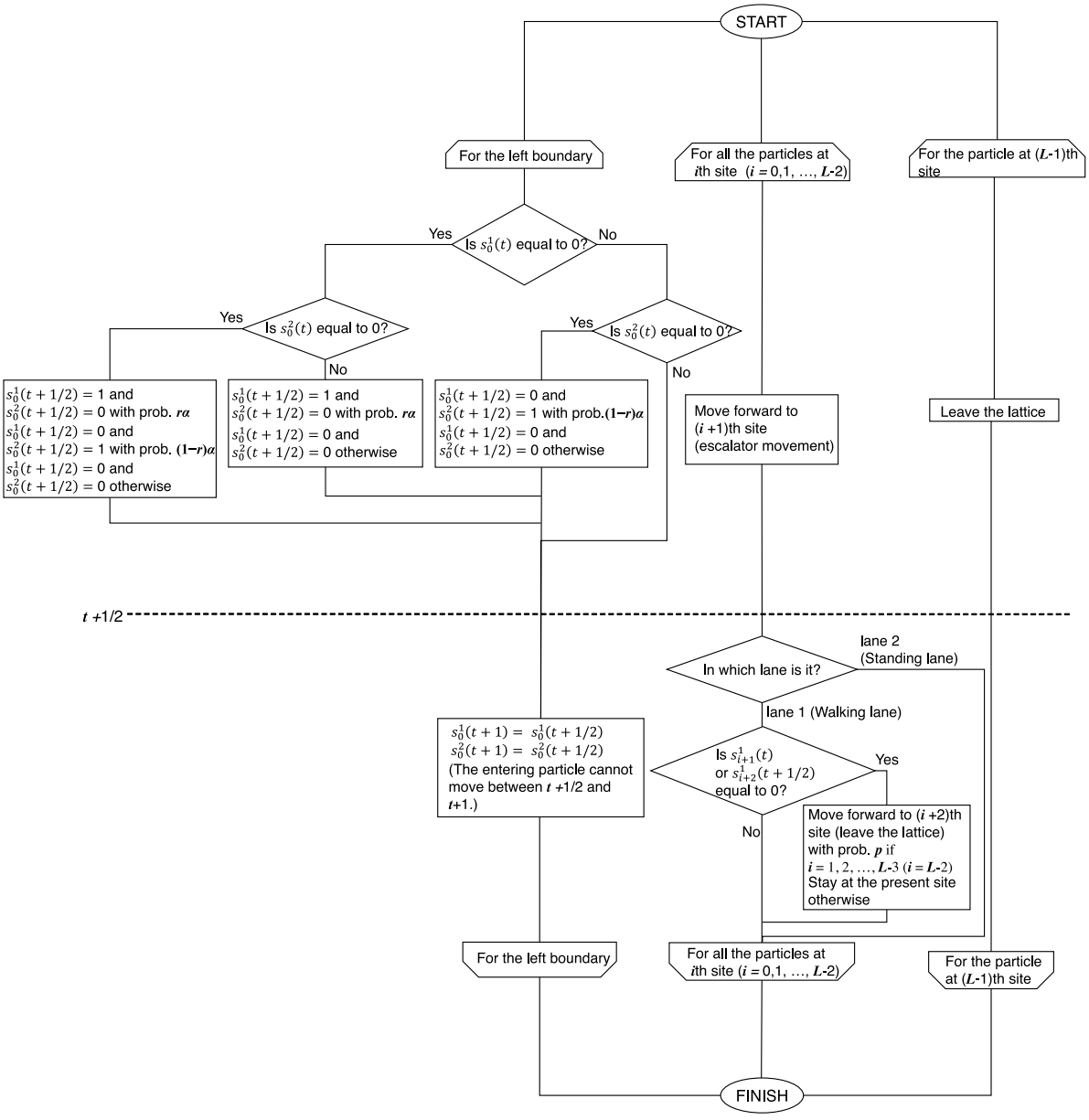

Fig. 3. Pseudo flow diagram for our model with Strategy SW from time t to $t+1$. Lane 1 and 2 correspond to a walking and standing lane, respectively. We note that with Strategy SS and WW the update flows are abbreviated because they are the simpler versions of that with Strategy SW.

4.1. Steady-state flow Q_{SS}, Q_{SW}, and Q_{WW}

Before examining T, we briefly discuss the steady-state flow in the two-lane model.

Since particles can always enter the system with Strategy SS and WW (see Section 2), the following relation holds

$$Q_{SS} = Q_{WW} = \alpha, \tag{3}$$

where Q_{SS} and Q_{WW} are defined as the steady-state flow of the two-lane model with Strategy SS and WW, respectively. We emphasize that counter-intuitively, $Q_{WW} = Q_{SS}$ because of the independence of the flow from p (see Section 3), so walking can have no effect on increasing the steady-state flow.

Second, with Strategy SW, particles prefer to enter a standing lane or a walking lane with some probability. Given that a particle prefers standing with probability $1-r$, the input probability of the standing lane reduces to $(1-r)\alpha$. Similarly,

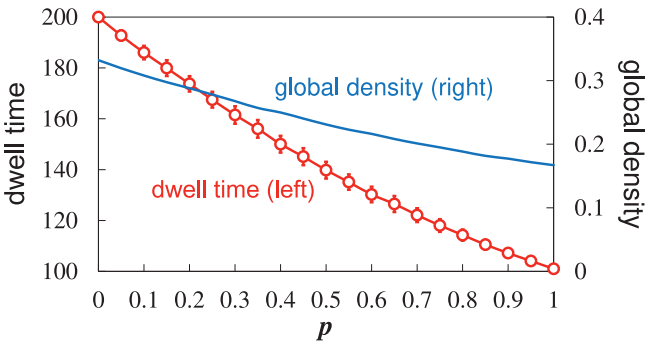

Fig. 4. Simulation values of dwell time (red, left axis) with the sample standard deviation and global density (blue, right axis) as functions of p. The dwell time is calculated by averaging the times of 1000 particles starting from the (10^4+1)th particle, and the global density calculated by averaging over 10^5 time steps after evolving the system for 10^4 time steps.

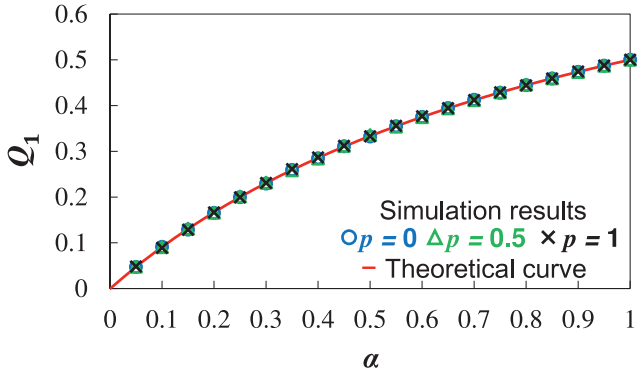

Fig. 5. Simulation (dots) and theoretical (curve) values of Q_1 as functions of α for various $p \in \{0$(blue circles), 0.5(green triangles), 1(black crosses)$\}$.

that of the walking lane reduces to $r\alpha$. Therefore, the steady-state flows of the standing lane Q_S and the walking lane Q_W in the two-lane model are given as

$$Q_S = \frac{(1-r)\alpha}{1+(1-r)\alpha}, \tag{4}$$

and

$$Q_W = \frac{r\alpha}{1+r\alpha}, \tag{5}$$

which are derived from Eq. (2) by replacing α with $(1-r)\alpha$ and $r\alpha$, respectively.

Consequently, the steady-state flow of the two-lane model with Strategy SW, Q_{SW}, can be calculated as

$$Q_{SW} = Q_S + Q_W = \frac{(1-r)\alpha}{1+(1-r)\alpha} + \frac{r\alpha}{1+r\alpha}, \tag{6}$$

which takes its maximum value when $r = 0.5$. The detailed properties of the function of Eq. (6) are discussed in Appendix A. Fig. 6 compares the simulation (dots) and theoretical (curves) values of (a) Q_{SS}, Q_{SW} for $p \in \{0.5, 1\}$, and Q_{WW} for $p \in \{0.5, 1\}$ as functions of α, and (b) Q_{SW} for various $\alpha \in \{0.2, 0.6, 1\}$ and $p \in \{0.5, 1\}$ as functions of r. The simulation values again show very good agreement with the theoretical curves.

From Eqs. (3) and (6), we immediately obtain

$$Q_{SW} < r\alpha + (1-r)\alpha = \alpha = Q_{SS}(= Q_{WW}), \tag{7}$$

indicating that Strategy SS (WW) is always advantageous in terms of steady-state flow.

The absolute advantage of Strategy SS (WW) over Strategy SW is explained with the behavior at the entrances of the lanes. Table 4 summarizes the model behavior at the left boundary, extracting the first and second site with $\alpha = 1$. With Strategy SS (WW), since consecutive pairs of particles mutually enter either lane, two particles can enter the system in two time steps, as shown in the upper panel of Table 4.

On the other hand, with Strategy SW they cannot enter the system with two time steps but with three time steps, if both of two consecutive particles' preference are the same, as shown in the lower panel of Table 4. The two particles can

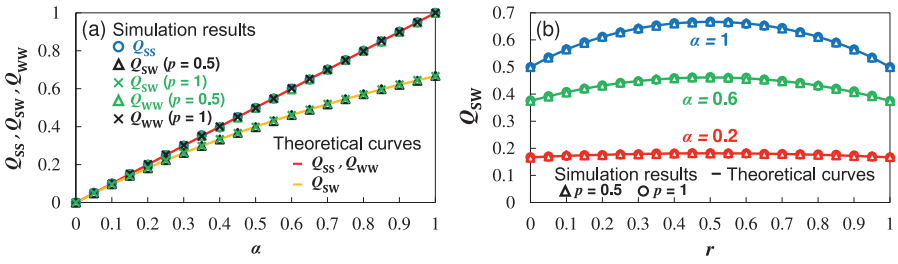

Fig. 6. Simulation (dots) and theoretical (red/orange curves) values of (a) Q_{SS} (blue circles), Q_{SW} for $p \in \{0.5$(black triangles), 1(green crosses)$\}$, and Q_{WW} for $p \in \{0.5$(green triangles), 1(black crosses)$\}$ as functions of α, and (b) Q_{SW} for various $\alpha \in \{0.2$(red), 0.6(green), 1(blue)$\}$ and $p \in \{0.5$(triangles), 1(circles)$\}$ as functions of r.

Table 4
Comparison of the left boundary between Strategy SS and SW, with constant $\alpha = 1$. Two red particles can enter either of two standing lanes with Strategy SS. Two green particles, which prefer walking in this figure, attempt to enter the walking lane with Strategy SW, not entering a standing lane. We note that the upper (lower) lane is a standing (walking) lane for Strategy SW.

Strategy	Time t	Time t+1	Time t+2
SS	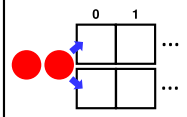	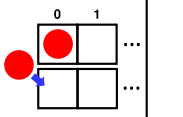	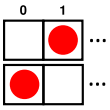
SW	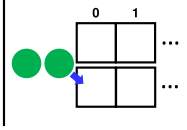	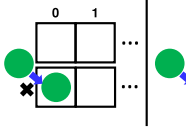	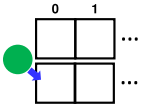

enter the system in two time steps if two consecutive particles separately prefer walking and standing. Therefore, Q_{SW} is maximized if $r = 0.5$, which clearly maximizes the probability that the preferences of the two consecutive particles differ.

Considering that the system is governed by the left boundary, these facts finally lead to $Q_{SS} > Q_{SW}$, explaining the absolute advantage of Strategy SS (WW) over Strategy SW. We note that two revised escalator models, discussed in Appendix B, also satisfy $Q_{SS} \geq Q_{SW}$, although Q_{SW} is improved.

4.2. Total (macro-scale) transportation time T

4.2.1. Approximate theoretical analyses of T

In this subsection, we theoretically calculate the approximations of T_{SS} (total transportation time with Strategy SS), T_{SW} (total transportation time with Strategy SW), and T_{WW} (total transportation time with Strategy WW) and consider the relations among them.

Considering that the steady-state flow Q expresses the average number of particles that pass a certain point (the left boundary) each time step, the average required time steps $T^s(N)$ for the Nth particle to enter the system from the time at which the first-entering particle enters in steady-state flow can be calculated as

$$T^s(N) \approx \frac{N-1}{Q}. \tag{8}$$

On the other hand, the required time steps $T^f(p)$ for the final-leaving particle of both lanes, which is not always identical to the final-entering particle, to reach the right boundary can be represented as

$$\begin{cases} T^f = T^f_S = \dfrac{L}{1} & \text{for a standing lane,} \\ T^f(p) = T^f_W(p) \gtrapprox \dfrac{L}{1+p} & \text{for a walking lane,} \end{cases} \tag{9}$$

where T^f_S (T^f_W) is a (an) definitive (approximate) value, and when calculating T^f_W the possibility that a walking-preference particle is blocked by the particle ahead of it is ignored, resulting in a slight underestimation of T^f_W (see also Section 4.2.2).

Assuming that (i) $1/\alpha$ time steps are needed on average for the first particle to enter the system, and that (ii) particles enter both lanes during the steady-state flow after the first particle enters the system, $T_{SS}(N, \alpha)$ and $T_{WW}(N, \alpha, p)$— their

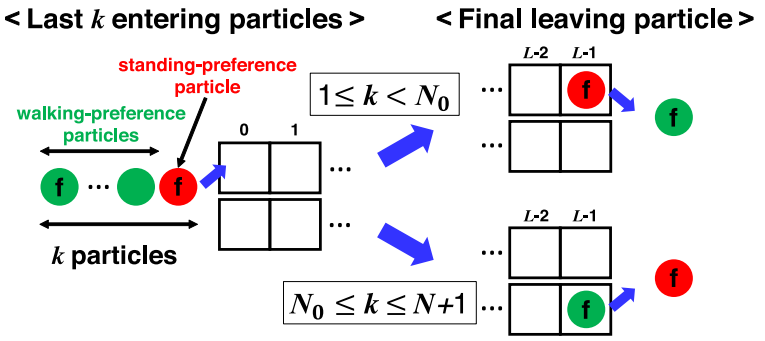

Fig. 7. Schematic illustration for explaining N_0. The red (green) particles are standing- (walking-preference) particles, and the red (green) particle labeled 'f' is the final-entering standing-preference (walking-preference) particle. If $1 \le k < N_0$, the final-leaving particle is, on average, identical to the final-entering standing-preference particle; otherwise the final-leaving particle is identical to the final-entering walking-preference particle.

arguments can be abbreviated unless otherwise specified (similarly for other variables)—can be written as

$$T_{\mathrm{SS}}(N,\alpha) \approx \frac{1}{\alpha} + T^{\mathrm{s}}_{\mathrm{SS}}(N) + T^{\mathrm{f}}_{\mathrm{S}} = \frac{N}{\alpha} + \frac{L}{1} \tag{10}$$

and

$$T_{\mathrm{WW}}(N,\alpha,p) \approx \frac{1}{\alpha} + T^{\mathrm{s}}_{\mathrm{WW}}(N) + T^{\mathrm{f}}_{\mathrm{W}} = \frac{N}{\alpha} + \frac{L}{1+p}, \tag{11}$$

from Eqs. (3), (8), and (9). We note that the first-in-first-out condition – i.e., the entering sequence is identical to the leaving sequence – must be satisfied when Strategy SS is modeled, whereas the relation is mostly satisfied when Strategy WW is modeled.

From Eqs. (10) and (11), T_{SS} and T_{WW} differ only due to the difference in the second term, resulting in $T_{\mathrm{SS}} \approx T_{\mathrm{WW}}$ if N is sufficiently large.

Under the same assumption, we then consider T_{SW}. Unlike T_{SS} and T_{WW}, the first-in-first-out condition generally does not hold since the hopping probabilities of the two lanes are different, leading to difficulty in calculating T_{SW}.

For approximate calculations of T_{SW}, we need to consider the final-entering standing-preference particle and the final-entering walking-preference one. Let us define N_0 as a threshold number. Specifically, if a standing-preference particle is (not) included in the last N_0 entering particles, the final leaving particle is on average identical to the final-entering standing-preference (walking-preference) particle. We note that if $r = 1$, N_0 is always $N_0 = 0$.

Fig. 7 gives a schematic illustration of N_0. This figure focuses on the last k entering particles, where the kth ($k = 1, \ldots, N+1$) entering particle from the final-entering particle is identical to the final-entering standing-preference particle. We note that $k = N+1$ represents that all N particles prefer walking, which is defined for the sake of convenience.

Similarly to the assumptions as those applied to T_{SS} and T_{WW}, if we assume that (iii) particles tend to enter the system every $1/Q_{\mathrm{SW}}$ time steps, and that (iv) a standing-preference (walking-preference) particle on average stays in the system for $L/1$ ($L/(1+p)$) time steps, N_0 satisfies

$$(N_0 - 1) \times \frac{1}{Q_{\mathrm{SW}}} \approx \frac{L}{1} - \frac{L}{1+p}. \tag{12}$$

Consequently, N_0 reduces to

$$N_0 \approx \left(\frac{L}{1} - \frac{L}{1+p}\right)\frac{1}{Q_{\mathrm{SW}}} + 1 = \frac{pL}{1+p}\left\{\frac{r\alpha}{1+r\alpha} + \frac{(1-r)\alpha}{1+(1-r)\alpha}\right\} + 1. \tag{13}$$

We note that although N_0 is defined to be a continuous value, we use its integer part when it is used as the upper limit of summation, which must be an integer.

Regarding T_{SW} as a random variable, i.e., $T_{\mathrm{SW}} = t_{\mathrm{SW}}(k)$ ($k = 1, 2, \ldots, N+1$), $t_{\mathrm{SW}}(k)$ can be represented as

$$t_{\mathrm{SW}}(k) \approx \begin{cases} \dfrac{1}{\alpha} + T^{\mathrm{s}}_{\mathrm{SW}}(N-k+1) + T^{\mathrm{f}}_{\mathrm{S}} & \text{for } 1 \le k < N_1, \\ \dfrac{1}{\alpha} + T^{\mathrm{s}}_{\mathrm{SW}}(N) + T^{\mathrm{f}}_{\mathrm{W}} & \text{for } N_1 \le k \le N+1, \end{cases} \tag{14}$$

where $N_1 = \min(N, N_0)$.

Because each particle prefers standing (walking) with probability $1-r$ (r), the probability $P(k)$ that the kth-entering particle from the final one is identical to the final-entering standing-preference particle can be calculated as

$$P(k)=\begin{cases}(1-r)r^{k-1} & \text{for } 1\le k\le N,\\ r^{k-1} & \text{for } k=N+1,\end{cases} \tag{15}$$

satisfying $\sum_{k=1}^{N+1}P(k)=1$.

Using Eqs. (14) and (15), the expected value of T_{SW} can be calculated as

$$\begin{aligned}T_{\mathrm{SW}} &\approx \sum_{k=1}^{N+1}P(k)t_{\mathrm{SW}}(k)\\ &=\frac{1}{\alpha}+\sum_{k=1}^{N_1}\{P(k)(T_{\mathrm{SW}}^{\mathrm{s}}(N-k+1)+T_{\mathrm{S}}^{\mathrm{f}})\}+\left(1-\sum_{k=1}^{N_1}P(k)\right)\times(T_{\mathrm{SW}}^{\mathrm{s}}(N)+T_{\mathrm{W}}^{\mathrm{f}})\\ &=\frac{1}{\alpha}+\frac{N-1}{Q_{\mathrm{SW}}}-\frac{\sum_{k=1}^{N_1}(1-r^{N_1-k})r^k}{Q_{\mathrm{SW}}}+\frac{(1-r^{N_1})L}{1}+\frac{r^{N_1}L}{1+p}\\ &=\frac{1}{\alpha}+\frac{N-1}{\frac{r\alpha}{1+r\alpha}+\frac{(1-r)\alpha}{1+(1-r)\alpha}}-\frac{\sum_{k=1}^{N_1}(1-r^{N_1-k})r^k}{\frac{r\alpha}{1+r\alpha}+\frac{(1-r)\alpha}{1+(1-r)\alpha}}+\frac{(1-r^{N_1})L}{1}+\frac{r^{N_1}L}{1+p}.\end{aligned} \tag{16}$$

The detailed derivation of T_{SW} is given in Appendix C.

Next, we compare T_{SS}, T_{SW}, and T_{WW}, using Eqs. (10), (11), and (16). First, T_{SS} clearly exceeds T_{WW}. In addition, T_{SW} also exceeds T_{WW} because of the following equation:

$$\begin{aligned}T_{\mathrm{SW}} &> \frac{1}{\alpha}+\sum_{k=1}^{N_1}\{P(k)(T_{\mathrm{SW}}^{\mathrm{s}}(N-N_1)+T_{\mathrm{S}}^{\mathrm{f}})\}+\left(1-\sum_{k=1}^{N_1}P(k)\right)(T_{\mathrm{SW}}^{\mathrm{s}}(N)+T_{\mathrm{W}}^{\mathrm{f}})\\ &=\frac{1}{\alpha}+\sum_{k=1}^{N_1}P(k)\left(\frac{N-1}{Q_{\mathrm{SW}}}-\frac{N_1}{Q_{\mathrm{SW}}}+\frac{L}{1}\right)+\left(1-\sum_{k=1}^{N_1}P(k)\right)\left(\frac{N-1}{Q_{\mathrm{SW}}}+\frac{L}{1+p}\right)\\ &\ge\frac{1}{\alpha}+\sum_{k=1}^{N_1}P(k)\left(\frac{N-1}{Q_{\mathrm{SW}}}-\frac{N_0}{Q_{\mathrm{SW}}}+\frac{L}{1}\right)+\left(1-\sum_{k=1}^{N_1}P(k)\right)\left(\frac{N-1}{Q_{\mathrm{SW}}}+\frac{L}{1+p}\right)\\ &=\frac{1}{\alpha}+\frac{N-1}{Q_{\mathrm{SW}}}+\frac{L}{1+p}\ge\frac{1}{\alpha}+\frac{N-1}{Q_{\mathrm{WW}}}+\frac{L}{1+p}=T_{\mathrm{WW}}.\end{aligned} \tag{17}$$

The relation between T_{SS} and T_{SW} is somewhat complicated. Using Eqs. (10) and (16), $T_{\mathrm{SW}}-T_{\mathrm{SS}}$ can be calculated as

$$\begin{aligned}T_{\mathrm{SW}}-T_{\mathrm{SS}} &=\frac{1}{\alpha}+\frac{N-1}{Q_{\mathrm{SW}}}-\frac{\sum_{k=1}^{N_1}(1-r^{N_1-k})r^k}{Q_{\mathrm{SW}}}+\frac{(1-r^{N_1})L}{1}+\frac{r^{N_1}L}{1+p}-\left(\frac{N}{Q_{\mathrm{SS}}}+\frac{L}{1}\right)\\ &=\underbrace{(N-1)\left(\frac{1}{Q_{\mathrm{SW}}}-\frac{1}{Q_{\mathrm{SS}}}\right)-\frac{\sum_{k=1}^{N_1}(1-r^{N_1-k})r^k}{Q_{\mathrm{SW}}}}_{\text{first part}}\underbrace{-\frac{pr^{N_1}}{1+p}\frac{L}{1}}_{\text{second part}}.\end{aligned} \tag{18}$$

First, the second part of Eq. (18) is always equal to or less than 0 (the equal sign holds only when $r=0$), and can be regarded as a function of L. This is due to the shorter dwell time of walking-preference particles compared to standing-preference particles (see also Fig. 4). We hereafter refer to this effect as the 'positive effect of walking,' and it disappears gradually as r decreases or N_1 increases, since $r^{N_1}\approx 0$.

On the other hand, the sign of the first part of Eq. (18) depends on the parameters. For $N>1$, the first term in the first part is always positive, due to $Q_{\mathrm{SS}}>Q_{\mathrm{SW}}$ (see Eq. (7)), and can be regarded as a function of N.

However, the existence of the second term in the first part of Eq. (18) leads to the result that the first part of Eq. (18) becomes negative. The numerator of this term satisfies the following relation:

$$\sum_{k=1}^{N_1}(1-r^{N_1-k})r^k<N_1(1-r^{N_1})<N_1. \tag{19}$$

From the definition of N_1, this numerator increases monotonically and converges to a constant value; specifically, $\sum_{k=1}^{N_0}(1-r^{N_0-k})r^k$ when $N\ge N_0$, as N increases. From Eq. (13), this constant value can be regarded as a monotonically increasing function of L.

Therefore, for sufficiently large N, the first part of Eq. (18) exceeds 0. We hereafter refer this effect as the 'negative effect of preference,' because a difference arises due to $Q_{\mathrm{SS}}>Q_{\mathrm{SW}}$, which is introduced by the walking/standing preference (see Eq. (7)).

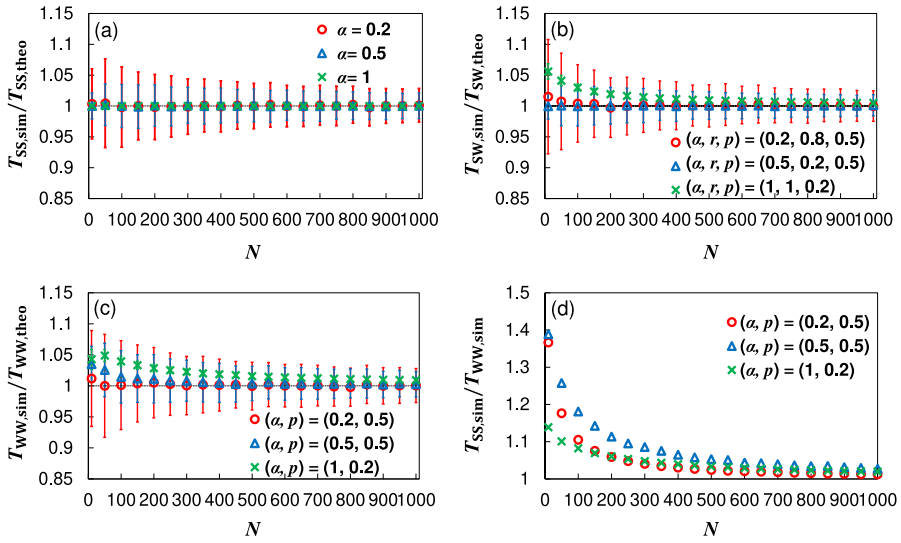

Fig. 8. Calculated values of the ratios (a) $T_{\mathrm{SS,sim}}/T_{\mathrm{SS,theo}}$ for $\alpha \in \{0.2$(red circles), 0.5(blue triangles), 1(green crosses)$\}$, (b) $T_{\mathrm{SW,sim}}/T_{\mathrm{SW,theo}}$ for various $(\alpha, r, p) \in \{(0.2, 0.8, 0.5)$(red circles), $(0.5, 0.2, 0.5)$(blue triangles), $(1, 1, 0.2)$(green crosses)$\}$, (c) $T_{\mathrm{WW,sim}}/T_{\mathrm{WW,theo}}$ for various $(\alpha, p) \in \{(0.2, 0.5)$(red circles), $(0.5, 0.5)$(blue triangles), $(1, 0.2)$(green crosses)$\}$, (d) $T_{\mathrm{SS,sim}}/T_{\mathrm{WW,sim}}$ for various $(\alpha, p) \in \{(0.2, 1)$(red circles), $(0.5, 0.5)$(blue triangles), $(1, 0.2)$(green crosses)$\}$. All the plots start from $N = 10$. The error bars in the plots of (a), (b), and (c) represent one sample standard deviation for 1000 trials.

Consequently, $T_{\mathrm{SW}} - T_{\mathrm{SS}}$ for $N > N_0$ can be rewritten as

$$T_{\mathrm{SW}} - T_{\mathrm{SS}} = f(N) - g(L), \tag{20}$$

where $f(N)$ and $g(L)$ are, respectively, monotonically increasing functions of N and L. This fact implies that for sufficiently large N the positive effect of walking becomes negligible and $T_{\mathrm{SW}} - T_{\mathrm{SS}} > 0$ ($T_{\mathrm{SW}} > T_{\mathrm{SS}}$), while this relation can be reversed for small N. From Eqs. (10) and (16), $T_{\mathrm{SW}}/T_{\mathrm{SS}}$ converges to a certain value as N increases, as

$$\lim_{N\to\infty} \frac{T_{\mathrm{SW}}}{T_{\mathrm{SS}}} = \lim_{N\to\infty} \frac{\frac{1}{\alpha} + \frac{N-1}{Q_{\mathrm{SW}}} - \frac{\sum_{k=1}^{N_1}(1-r^{N_1-k})r^k}{Q_{\mathrm{SW}}} + \frac{(1-r^{N_1})L}{1} + \frac{r^{N_1}L}{1+p}}{\frac{N}{Q_{\mathrm{SS}}} + \frac{L}{1}} = \lim_{N\to\infty} \frac{\frac{N-1}{Q_{\mathrm{SW}}}}{\frac{N}{Q_{\mathrm{SS}}}} = \frac{Q_{\mathrm{SS}}}{Q_{\mathrm{SW}}} > 1. \tag{21}$$

The discussion in this subsection indicates that (i) Strategy WW is always advantageous over Strategy SS and SW, and that (ii) Strategy SS is advantageous over Strategy SW if N is sufficiently large; otherwise Strategy SW performs better than Strategy SS.

4.2.2. Validation of approximations of T

This subsection discusses the validity of the theoretical approximations of T_{SS}, T_{SW}, and T_{WW} by comparing them with the results of the numerical simulations.

Fig. 8 plots the calculated values of the ratios (a) $T_{\mathrm{SS,sim}}/T_{\mathrm{SS,theo}}$ for various $\alpha \in \{0.2, 0.5, 1\}$, (b) $T_{\mathrm{SW,sim}}/T_{\mathrm{SW,theo}}$ for various $(\alpha, r, p) \in \{(0.2, 0.8, 0.5), (0.5, 0.2, 0.5), (1, 1, 0.2)\}$, (c) $T_{\mathrm{WW,sim}}/T_{\mathrm{WW,theo}}$ for various $(\alpha, p) \in \{(0.2, 0.5), (0.5, 0.5), (1, 0.2)\}$, and (d) $T_{\mathrm{SS,sim}}/T_{\mathrm{WW,sim}}$ for various $(\alpha, p) \in \{(0.2, 0.5), (0.5, 0.5), (1, 0.2)\}$ as functions of N. We average the simulation values of T over 1000 trials (and do similarly below for the simulations of T unless otherwise specified).

Fig. 8(a) shows that the simulation values of T_{SS} agree with the theoretical ones very well, even for small N. Conversely, Fig. 8(b) and (c) show that the simulation values of T_{SW} and T_{WW} agree with the theoretical ones very well for large N; however, the simulation diverges from the analyses for small N and especially if p is small. This behavior can be explained as follows.

From Eq. (9), $T_{\mathrm{S}}^{\mathrm{f}}$ is a deterministic value, whereas $T_{\mathrm{W}}^{\mathrm{f}}$ is an expected one. In addition, although the final-leaving particle is assumed to be able to hop forward freely in the theoretical calculations, it may be blocked by the particle ahead of it in a walking lane, so $T_{\mathrm{W}}^{\mathrm{f}} > L/(1+p)$. These features mean that T_{SW} and T_{WW} can diverge in the theoretical approximations, especially for small N and small p, as these conditions enhance the influence of $T_{\mathrm{W}}^{\mathrm{f}}$ on T_{SW} and T_{WW}.

In Fig. 8(d), T_{SS} is confirmed to approach T_{WW} as N increases (strictly speaking, $T_{\mathrm{WW}} > T_{\mathrm{SS}}$). From here on, we do not consider T_{WW}, since $T_{\mathrm{WW}} < T_{\mathrm{SS}}$ and $T_{\mathrm{WW}} < T_{\mathrm{SW}}$, because of the difference in T^{f}.

4.3. Effect of N

In this subsection, we investigate the effect of N on T for various r. We set $\alpha = 0.5$ and $p = 0.5$ (in a walking lane).

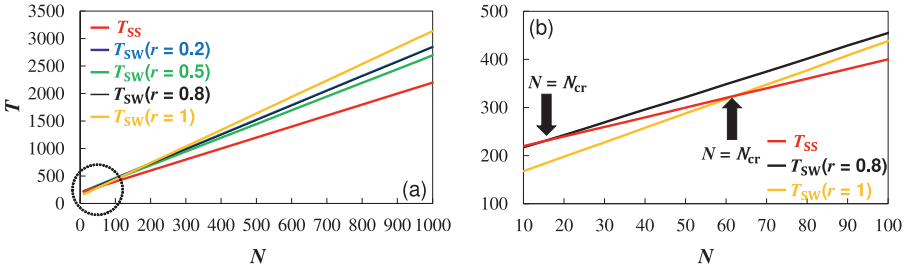

Fig. 9. (a) Simulation values of T_{SS} (red) and T_{SW} for various $r \in \{0.2(\text{blue}), 0.5(\text{green}), 0.8(\text{black}), 1(\text{yellow})\}$ as functions of N, fixing $\alpha = 0.5$ and $p = 0.5$. All the plots start from $N = 10$. (b) Zoomed Fig. 9(a), in the area enclosed with a black dotted circle in Fig. 9(a). We note that the curves for $r = 0.2$ and $r = 0.5$ are abbreviated. We visually mark the vicinities of $N = N_{cr}$, which will be discussed in Section 4.7, with black arrows.

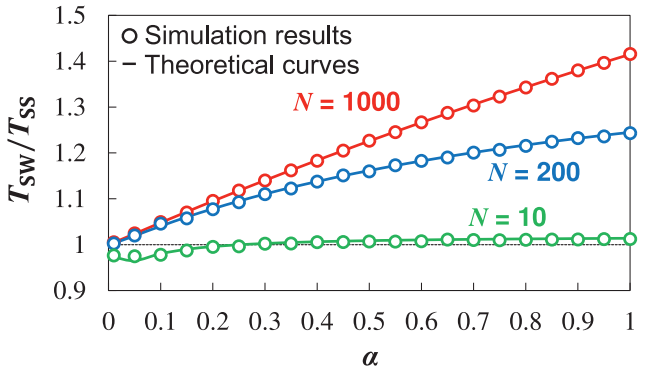

Fig. 10. Simulation (circles) and theoretical (curves) values of the ratio T_{SW}/T_{SS} as functions of α for various $N \in \{10(\text{green}), 200(\text{blue}), 1000(\text{red})\}$. The other parameters are fixed as $r = 0.5$ and $p = 0.5$, respectively. All the plots start from $\alpha = 0.01$.

Fig. 9(a) compares T_{SS} and T_{SW} for various $r \in \{0.2, 0.5, 0.8, 1\}$ as functions of N and Fig. 9(b) is a zoomed-in inset of Fig. 9(a). In Fig. 9(a), we can observe that T_{SW} generally exceeds T_{SS} at least for $N > 100$. This trend means that the negative effect of preference is always greater than the positive effect of walking for large N. Moreover, $T_{SW} - T_{SS}$ increases as N becomes greater. This phenomenon is expected from Eq. (20). We note that the curves for $r = 0.2$ and $r = 0.8$ mostly overlap, even though they are, strictly speaking, different (see also Eq. (16))—because the steady-state flows are the same.

On the other hand, in Fig. 9(b), some cases of $T_{SS} > T_{SW}$ appear for small N, especially for relatively large r. This behavior is because in those limited cases, T_{SW} is influenced very much by the positive effect of walking, i.e., r^{N_1} is relatively large.

4.4. Effect of α

In this subsection, we investigate the effect of α on T for various N. We set $r = 0.5$, and $p = 0.5$ (in a walking lane).

Fig. 10 compares the simulation (circles) and theoretical (curves) values for the ratio T_{SW}/T_{SS} as functions of α for various $N \in \{10, 200, 1000\}$. The simulation results show very good agreement with the theoretical curves. The inequality $T_{SW}/T_{SS} > 1$ ($T_{SW}/T_{SS} < 1$) means that Strategy SS (Strategy SW) is advantageous. In Fig. 10, again we see that $T_{SW}/T_{SS} > 1$ ($T_{SS} < T_{SW}$) regardless of α for large N ($N = 200$ and 1000 in this figure).

On the other hand, T_{SW}/T_{SS} decreases as α decreases, and T_{SW}/T_{SS} can become less than 1 ($T_{SS} > T_{SW}$) for small α and small N ($N = 10$ and $\alpha < 0.2$ in this figure). This trend is explained as follows.

From Eqs. (3), (6), and (21) we obtain

$$\lim_{N\to\infty} \frac{T_{SW}}{T_{SS}} = \frac{Q_{SS}}{Q_{SW}} = \frac{1}{\frac{r}{1+r\alpha} + \frac{1-r}{1+(1-r)\alpha}}, \tag{22}$$

which increases monotonically with respect to α. Therefore, for sufficiently large N, T_{SW}/T_{SS} increases (decreases) as α increases (decreases).

Then, taking note of the following two relations:

$$\lim_{\alpha\to 0} \frac{Q_{SW}}{Q_{SS}} = \lim_{\alpha\to 0} \left\{ \frac{r}{1+r\alpha} + \frac{1-r}{1+(1-r)\alpha} \right\} = 1 \tag{23}$$

and

$$\lim_{\alpha\to 0} N_1 = \lim_{\alpha\to 0} N_0 = \lim_{\alpha\to 0}\left[\frac{pL}{1+p}\left\{\frac{r\alpha}{1+r\alpha}+\frac{(1-r)\alpha}{1+(1-r)\alpha}\right\}+1\right] = 1, \tag{24}$$

we have

$$\begin{aligned}\lim_{\alpha\to 0}\frac{T_{SW}}{T_{SS}} &= \lim_{\alpha\to 0}\frac{\frac{1}{\alpha}+\frac{N-1}{Q_{SW}}-\frac{\sum_{k=1}^{N_1}(1-r^{N_1-k})r^k}{Q_{SW}}+\frac{(1-r^{N_1})L}{1}+\frac{r^{N_1}L}{1+p}}{\frac{N}{Q_{SS}}+\frac{L}{1}}\\ &= \lim_{\alpha\to 0}\frac{N-\sum_{k=1}^{N_1}(1-r^{N_1-k})r^k+\frac{\alpha(1-r^{N_1})L}{1}+\frac{\alpha r^{N_1}L}{1+p}}{N+\frac{\alpha L}{1}}\\ &= \lim_{\alpha\to 0}\left\{1-\frac{\sum_{k=1}^{N_1}(1-r^{N_1-k})r^k}{N}\right\} = 1.\end{aligned} \tag{25}$$

In Fig. 10, all the plots (curves) are observed to approach 1 as α approaches 0. Eq. (23) implies that for small α, the negative effect of preference disappears.

Here, we define a new value $\alpha = \alpha_1$, where α_1 ($0 < \alpha_1 \le 1$) satisfies

$$N_0(\alpha = \alpha_1) = 2 \Leftrightarrow \frac{pL}{1+p}\left\{\frac{r\alpha_1}{1+r\alpha_1}+\frac{(1-r)\alpha_1}{1+(1-r)\alpha_1}\right\} = 1. \tag{26}$$

For sufficiently large N, $T_{SW} - T_{SS}$ always exceeds 0 when $\alpha_1 < \alpha \le 1$, which is discussed in detail in Appendix D.

On the other hand, when $0 < \alpha \le \alpha_1$, from Eq. (18),

$$T_{SW} - T_{SS} = (N-1)\left(\frac{1}{Q_{SW}}-\frac{1}{Q_{SS}}\right)-\frac{rp}{1+p}\frac{L}{1} = \frac{N-1}{Q_{SW}}\times h(\alpha) > 0, \tag{27}$$

where $h(\alpha)$ is defined as

$$h(\alpha) = 1-\frac{Q_{SW}}{Q_{SS}}-\frac{rpLQ_{SW}}{(1+p)(N-1)}. \tag{28}$$

The behavior of $h(\alpha)$ is discussed in detail in Appendix E. We note that $N_1 = N_0 = 1$ for the upper limit of summation when $\alpha \le \alpha_1$. Eq. (27) indicates that for sufficiently large N; especially,

$$N > \frac{pL}{1+p}\max\left(\frac{r}{1-r}, 1\right)+1, \tag{29}$$

T_{SW}/T_{SS} always exceeds 1, and converges to 1 with $\alpha \to 0$, because the negative effect of preference is always greater than the positive effect of walking when $0 < \alpha \le 1$.

On the other hand, for small N, as α decreases, T_{SW}/T_{SS} can become below 1, because the positive effect of walking is greater than the negative effect of walking, and finally T_{SW}/T_{SS} converges to 1 from Eq. (25).

4.5. Effect of r

In this subsection, we investigate the effect of r on T_{SW} for various N. We set $\alpha = 0.5$ and $p = 0.5$ (in a walking lane). We note that only the standing (walking) lane is used and the other lane is always vacant if $r = 0$ ($r = 1$).

Fig. 11 compares the simulation (circles) and theoretical (curves) values of the ratio T_{SW}/T_{SS} as functions of r for various $N \in \{10, 200, 1000\}$. We emphasize that T_{SS} is constant for all values of r. The simulation results again show very good agreement with the theoretical curves even though they diverge in very limited cases of small N and large r ($N = 10$ and $r > 0.7$ in this figure).

This divergence can be explained as follows. First, the positive effect of walking is dominant for small N and large r, since the influence of the negative effect of preference is small and r^{N_1} approaches 1. In addition, although the final leaving particle is assumed to be able to hop forward freely in the theoretical calculations, it can be blocked by the particle ahead of it in a walking lane, leading to a slight underestimation of T_{SW} (see Section 4.2.2). Consequently, small N and large r enhance the influence of $L/(1+p)$ and increase the likelihood of underestimating it when calculating the theoretical values of T_{SW}, so the theoretical curve remains below the simulation values.

In Fig. 11, we see that $T_{SW}/T_{SS} > 1$ ($T_{SS} < T_{SW}$) for large N ($N = 200$ and 1000 in this figure) regardless of r, whereas $T_{SW}/T_{SS} < 1$ ($T_{SS} > T_{SW}$) for small N and large r ($N = 10$ and $r > 0.7$ in this figure).

In addition, we also note that T_{SW}/T_{SS} takes its minimum value near $r = 0.5$ for sufficiently large N ($N = 200$ and $N = 1000$ in this figure), because the negative effect of preference is least active with r being slightly more than 0.5, due to the positive effect of walking.

On the other hand, T_{SW}/T_{SS} can take a minimum value with $r = 1$ for sufficiently small N ($N = 10$ in this figure), due to the enhanced positive effect of walking for small N and large r. Due to the positive effect of walking, $T_{SW}/T_{SS}(r = 0) > T_{SW}/T_{SS}(r = 1)$ even for large N.

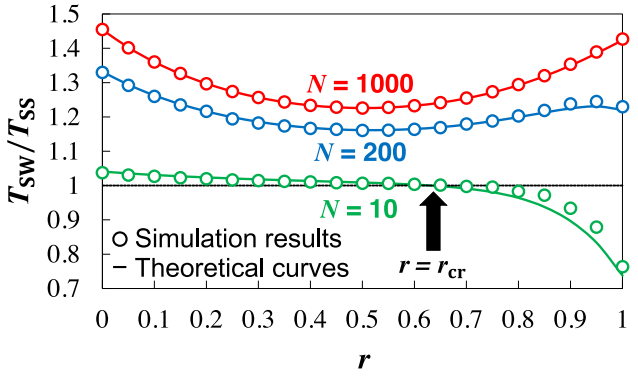

Fig. 11. Simulation (circles) and theoretical (curves) values of the ratio T_{SW}/T_{SS} as functions of r for various $N \in \{10(\text{green}), 200(\text{blue}), 1000(\text{red})\}$. The other parameters are fixed as $\alpha = 0.5$ and $p = 0.5$, respectively. We visually mark the vicinities of $r = r_{cr}$, which will be discussed in Section 4.7, with black arrows.

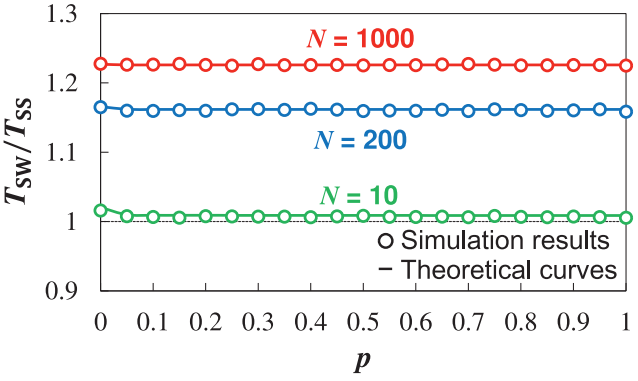

Fig. 12. Simulation (circles) and theoretical (curves) values of T_{SW}/T_{SS} as functions of p for various $N \in \{10(\text{green}), 200(\text{blue}), 1000(\text{red})\}$. The other parameters are fixed as $\alpha = 0.5$ and $r = 0.5$, respectively.

4.6. Effect of p

In this subsection, we investigate the effect of p (in a walking lane) on T_{SW} for various N. We set $\alpha = 0.5$, and $r = 0.5$. We emphasize that T_{SS} is constant regardless of p, as it is when changing r.

Fig. 12 plots the simulation (circles) and theoretical (curves) values of T_{SW}/T_{SS} as functions of p for various $N \in \{10, 200, 1000\}$. The simulation values again show very good agreement with the theoretical curves. In Fig. 12, we see that $T_{SW}/T_{SS} > 1$ ($T_{SS} < T_{SW}$) and T is hardly affected by p, because the steady-state flow does not depend on p and the positive effect of walking is very slight when $r = 0.5$ and $N \geq 10$.

We note that $T_{SW}/T_{SS} \neq 1$ ($T_{SS} \neq T_{SW}$) with $p = 0$, at which both lanes act as standing lanes even when Strategy SW is modeled. In this case, particles can enter either lane indiscriminately with Strategy SS, while particles still prefer either lane when Strategy SW is modeled.

4.7. Reversal point N_{cr} and r_{cr}

In this subsection, we theoretically determine $N_{cr}(\alpha, r, p)$ and $r_{cr}(N)$, at which $T_{SS} = T_{SW}$ (see also Figs. 9–11). These theoretical values are then compared with the simulation values.

From Eqs. (10) and (16), N_{cr} for $0 < r < 1$ satisfies the following relation:

$$T_{SS}(N = N_{cr}) = T_{SW}(N = N_{cr}) \tag{30}$$
$$\Leftrightarrow \frac{N_{cr}}{\alpha} + \frac{L}{1} = \frac{1}{\alpha} + \frac{N_{cr} - 1}{\frac{r\alpha}{1+r\alpha} + \frac{(1-r)\alpha}{1+(1-r)\alpha}} + \frac{(1-r^{N_1})L}{1} + \frac{r^{N_1}L}{1+p} - \frac{\frac{r}{1-r}\{1 - N_1 r^{N_1-1} + (N_1 - 1)r^{N_1}\}}{\frac{r\alpha}{1+r\alpha} + \frac{(1-r)\alpha}{1+(1-r)\alpha}},$$

where $N_1 = \min(N, N_0) = \min(N_{cr}, N_0)$. N_{cr} is generally difficult to obtain for $0 < r < 1$; however, for the case $r = 1$, the general form of N_{cr} can be obtained easily as

$$T_{SS}(N = N_{cr}) = T_{SW}(N = N_{cr}) \tag{31}$$

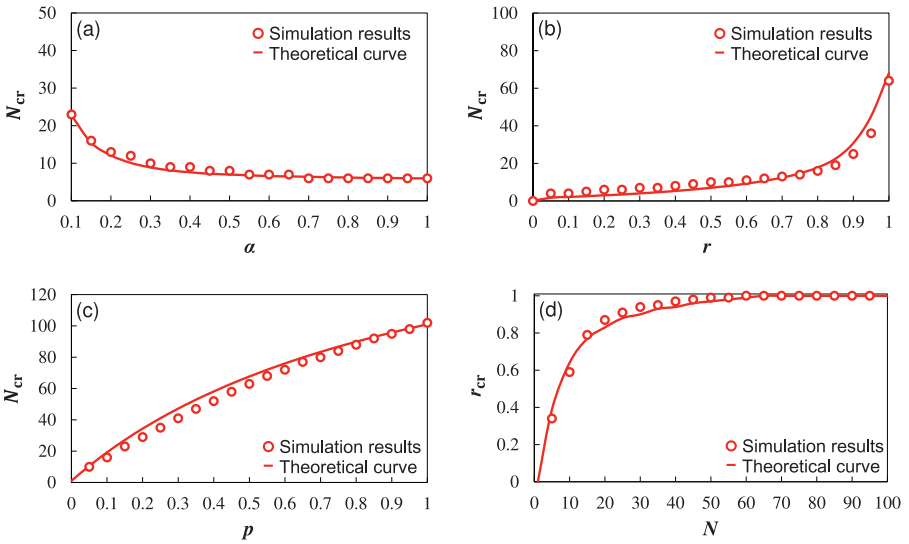

Fig. 13. Simulation (circles) and theoretical (curve) values of (a) N_{cr} as a function of α with $(r, p) = (0.5, 0.5)$, (b) N_{cr} as a function of r with $(\alpha, p) = (0.5, 0.5)$, (c) N_{cr} as a function of p with $(\alpha, r) = (0.5, 1)$, and (d) r_{cr} as a function of N with $(\alpha, p) = (0.5, 0.5)$. We note that the simulation values of N_{cr} satisfy $T_{SS}(N = N_{cr}) > T_{SW}(N = N_{cr})$ and $T_{SS}(N = N_{cr} + 1) < T_{SW}(N = N_{cr} + 1)$, and that those of r_{cr} satisfy $T_{SS}(r = r_{cr}) < T_{SW}(r = r_{cr})$ and $T_{SS}(r = r_{cr} + 0.01) > T_{SW}(r = r_{cr} + 0.01)$, if it exists.

$$\Leftrightarrow \frac{N_{cr}}{\alpha} + \frac{L}{1} = \frac{1}{\alpha} + \frac{N_{cr} - 1}{\frac{\alpha}{1+\alpha}} + \frac{L}{1+p} \Leftrightarrow N_{cr} = \frac{pL}{1+p} + 1.$$

Similarly, r_{cr} $(0 < r_{cr} < 1)$ satisfies the following relation:

$$T_{SS}(r = r_{cr}) = T_{SW}(r = r_{cr}) \tag{32}$$
$$\Leftrightarrow \frac{N}{\alpha} + \frac{L}{1} = \frac{1}{\alpha} + \frac{N-1}{\frac{r_{cr}\alpha}{1+r_{cr}\alpha} + \frac{(1-r_{cr})\alpha}{1+(1-r_{cr})\alpha}} + \frac{(1-{r_{cr}}^{N_1})L}{1} + \frac{r_{cr}^{N_1}L}{1+p} - \frac{\frac{r_{cr}}{1-r_{cr}}\{1 - N_1 r_{cr}^{N_1-1} + (N_1-1)r_{cr}^{N_1}\}}{\frac{r_{cr}\alpha}{1+r_{cr}\alpha} + \frac{(1-r_{cr})\alpha}{1+(1-r_{cr})\alpha}}.$$

We note that $r_{cr} = 1$ if no value in $0 < r_{cr} < 1$ that satisfies Eq. (32) exists, indicating that Strategy SS is always advantageous regardless of r for a fixed N.

Fig. 13 compares the simulation (circles) and theoretical (curves) values of (a) N_{cr} as a function of α, (b) N_{cr} as a function of r, (c) N_{cr} as a function of p, and (d) r_{cr} as a function of N. When calculating N_{cr} and r_{cr}, the simulation values of T were obtained as averages taken over 10^4 trials. In all figures, the simulations agree well with the theoretical curves.

From the definition of N_{cr} (r_{cr}), $T_{SS} > T_{SW}$, i.e., Strategy SW is advantageous, if $N < N_{cr}$ $(r > r_{cr})$; otherwise $T_{SS} < T_{SW}$ (Strategy SS is advantageous), for fixed (α, r, p) (for fixed (N, α, p)). Therefore, these results indicate that Strategy SS is generally advantageous especially for large N; however, in limited cases Strategy SW can perform better than Strategy SS, mainly for small α, large r, large p, and small N.

5. Individual (micro-scale) transportation time with the two-lane model

Now, we introduce the important novel quantity $\tau(n, \alpha, r, p)$. The quantity τ is defined as the time gap between the start of the simulation and the time when the nth-leaving particle leaves the system, which we refer to as the individual transportation time. The individual transportation times with Strategy SS and SW are represented as τ_{SS} and τ_{SW}, respectively, as when we were discussing T.

The quantity $\tau_{SS}(n)$ clearly coincides with $T_{SS}(N = n)$ as the first-in-first-out condition is always satisfied with Strategy SS; however, $\tau_{SW}(n)$ is generally below $T_{SW}(N = n)$ since the first-in-first-out condition might not hold with Strategy SW. We note that $\tau_{SW}(n) = T_{SW}(N = n)$ only for $r = 0$ and $r = 1$, for which the first-in-first-out condition must be satisfied, so r is set to $0 < r < 1$ in the following discussion.

5.1. Approximate theoretical analyses of n_{cr}

In this subsection, we theoretically determine approximate values for n_{cr}, for which $\tau_{SS}(n = n_{cr}) = \tau_{SW}(n = n_{cr})$.

Table 5
States (flows) of the system at ranges of time steps. 'Stand,' 'Walk,' and 'Entire' represent the standing lane, walking lane, and entire system, respectively. In addition, the notations 'R.P.' and 'S.S.' stand relaxation process and steady state, respectively.

No.	Time	Stand	Walk	Entire
1	$0 \le t < \frac{1}{\alpha} + \frac{L}{1+p}$	R.P. (0)	R.P. (0)	R.P. (0)
2	$\frac{1}{\alpha} + \frac{L}{1+p} \le t < \frac{1}{\alpha} + \frac{L}{1}$	R.P. (0)	S.S. (Q_W)	R.P. (Q_W)
3	$\frac{1}{\alpha} + \frac{L}{1} \le t$	S.S. (Q_S)	S.S. (Q_W)	S.S. (Q_{SW})

Unlike we did when approximating T, we regard the steady-state flow Q as the average number of particles that pass the right boundary in each step. In addition, we assume that (i) $1/\alpha$ time steps are needed on average for the first-entering standing-preference (walking-preference) particle to enter the system,[2] and that (ii) particles leave the system in the steady state after the first-leaving particle leaves the system. Furthermore, the number of particles is assumed to be sufficiently large. Especially, the number of all walking-preference particles needs to be larger than the average number of walking-preference particles that leave the system until the time at which the first-leaving standing-preference particle leaves the system.

We next define the threshold $n = n_2$; specifically, the n_2th-leaving walking-preference particle leaves the system approximately at the same time when the first-leaving standing-preference particle leaves. Therefore, n_2 satisfies

$$(n_2 - 1) \times \frac{1}{Q_W} \approx \frac{1}{\alpha} + \frac{L}{1} - \frac{1}{\alpha} - \frac{L}{1+p}, \tag{33}$$

which reduces to

$$n_2 \approx \frac{r\alpha}{1+r\alpha}\frac{pL}{1+p} + 1. \tag{34}$$

Based on the above assumptions, the system behavior can be in three states; (i) both lanes are not yet in steady state, (ii) only the walking lane is in steady state, and (iii) both lanes are in steady state. Table 5 summarizes the states (flows) of the system and relates them to time steps in terms of the model parameters.

Consequently, if we note the first n_2 particles leave the system with Q_W and the next $(n - n_2)$ particles leave with Q_{SW}, τ_{SW} reduces to

$$\tau_{SW}(n, \alpha, r, p) \approx \begin{cases} \dfrac{1}{\alpha} + \dfrac{L}{1+p} + \dfrac{n-1}{\frac{r\alpha}{1+r\alpha}} & \text{for } n \le n_2, \\ \dfrac{1}{\alpha} + \dfrac{L}{1} + \dfrac{n-n_2}{\frac{r\alpha}{1+r\alpha} + \frac{(1-r)\alpha}{1+(1-r)\alpha}} & \text{for } n > n_2, \end{cases} \tag{35}$$

from Eqs. (5) and (6).

On the other hand, since $\tau_{SS}(n) = T_{SS}(N = n)$, $\tau_{SS}(n, \alpha, p)$ can be written as

$$\tau_{SS}(n, \alpha, p) = T_{SS}(N = n) \approx \frac{L}{1} + \frac{n}{\alpha}, \tag{36}$$

from Eq. (10). From the definition of n_{cr}, and Eqs. (35) and (36), n_{cr} satisfies the following equation:

$$\tau_{SS}(n = n_{cr}) = \tau_{SW}(n = n_{cr}) \Leftrightarrow \frac{L}{1} + \frac{n_{cr}}{\alpha} = \frac{1}{\alpha} + \frac{L}{1} + \frac{n_{cr} - n_2}{\frac{r\alpha}{1+r\alpha} + \frac{(1-r)\alpha}{1+(1-r)\alpha}}. \tag{37}$$

The quantity τ_{SW} is clearly smaller than τ_{SS} for $n < n_2$, so $n_{cr} > n_2$. Therefore, $n_{cr}(\alpha, r, p)$ finally reduces to

$$n_{cr}(\alpha, r, p) = \frac{pLr\alpha\{1 + (1-r)\alpha\}}{[\{(1-r)^2 + r^2\}\alpha + r(1-r)\alpha^2](1+p)} + 1, \tag{38}$$

using Eqs. (34) and (37).

5.2. Comparison with simulation results

In this subsection, we compare the theoretical values, obtained in the previous subsection, with simulation ones.

[2] Strictly speaking, these required time steps for each lane are different; however, they are basically small unless r approaches very near 0 or 1. Therefore, we simply assume that they are equal to make the calculations easier.

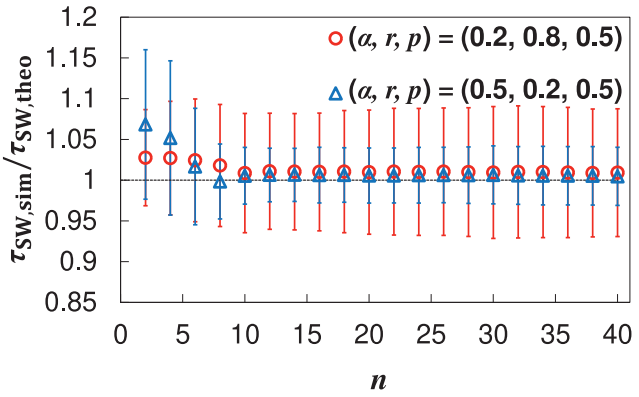

Fig. 14. Calculated values of the ratio $\tau_{\mathrm{SW,sim}}/\tau_{\mathrm{SW,theo}}$ as functions of n for $(\alpha, r, p) \in \{(0.2, 0.8, 0.5)$(red circles), $(0.5, 0.2, 0.5)$(blue triangles)$\}$ with fixed $N = 1000$. Both plots begin at $n = 2$. The error bars represent one sample standard deviation for 1000 trials.

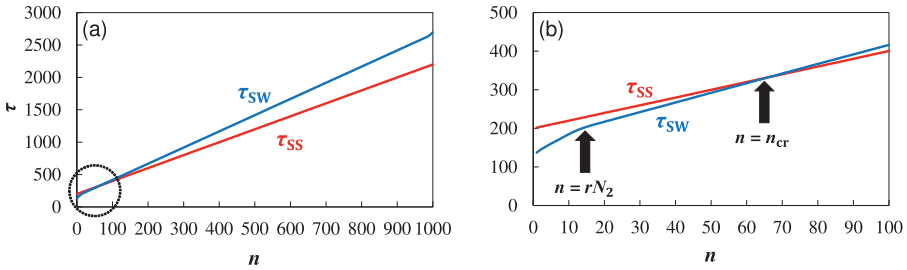

Fig. 15. (a) Simulation values of τ_{SS} (red) and τ_{SW} (blue) as functions of n, with fixed $\alpha = 0.5$, $r = 0.5$, $p = 0.5$, and $N = 1000$. (b) Zoomed-in inset Fig. 15(a), focusing on the range enclosed by a black dotted circle in Fig. 15(a). The vicinities of $n = rn_2$ and $n = n_{\mathrm{cr}}$ are marked with black arrows, respectively.

First, Fig. 14 shows the values of the ratio $\tau_{\mathrm{SW,sim}}/\tau_{\mathrm{SW,theo}}$ as functions of n for $(\alpha, r, p) \in \{(0.2, 0.8, 0.5), (0.5, 0.2, 0.5)\}$ with fixed $N = 1000$. The simulation values show very good agreement with the theoretical ones for $n > 10$. We note that the comparison regarding τ_{SS} is abbreviated since $\tau_{\mathrm{SS}}(n) = T_{\mathrm{SS}}(N = n)$.

Next, Fig. 15 compares the simulation values of τ_{SS} and τ_{SW} as functions of n, with fixed $N = 1000$. In Fig. 15(a) and (b), we see a point $\tau_{\mathrm{SS}}(n) = \tau_{\mathrm{SW}}(n)$, in which n is defined as $n = n_{\mathrm{cr}}$. This phenomenon can be explained qualitatively as follows.

At first, some of the first entering walking-preference particles leave the system when Strategy SW is simulated more quickly than when Strategy SS is simulated. In this case, for small n the positive effect of walking has the dominant effect on τ_{SW}, so $\tau_{\mathrm{SS}} > \tau_{\mathrm{SW}}$. After some time has elapsed, the negative effect of preference becomes dominant, resulting in $\tau_{\mathrm{SS}} < \tau_{\mathrm{SW}}$.

We then investigate the results of Fig. 15 in more microscopic ways. We first define the ratio x_m of the mth-entering particle in one trial as follows:

$$x_m = \frac{\tau_{\mathrm{SW,sim}}(n)}{\tau_{\mathrm{SS,theo}}(m)}, \tag{39}$$

where the mth-entering particle leaves the system in the nth with Strategy SW (generally $m \neq n$) and $\tau_{\mathrm{SS,theo}}(m)$ represents τ of the particle if Strategy SS was adopted. From the definition of x_m, the cases of $x_m < 1$ ($x_m > 1$) indicate that Strategy SW is effective (detrimental) for the particle.

We here divide $N(= 1000)$ particles into two groups; specifically, the first entering 100 particles (Group 1) and the other 900 ones (Group 2). Then, we average x_m for walking- and standing-preference particles in each group (the average is defined as $\bar{x}$). Fig. 16 plots the calculated values of $\bar{x}$ for the two groups with $(\alpha, r, p) \in \{$(a)$(0.2, 0.8, 0.5)$, (b)$(0.5, 0.2, 0.5)\}$.

In Fig. 16(a) and (b), $\bar{x}$ becomes below 1 only for the walking-preference particles in Group 1; otherwise, it exceeds 1. This fact indicates that the some walking-preference particles entering in the beginning benefit from Strategy SW; however, all the standing-preference particles and the rest of the walking-preference particles suffer a loss from Strategy SW.

Finally, Fig. 17 compares the simulation (dots) and theoretical (curve) values for n_{cr} as a function of r. In Fig. 17, the simulation values show relatively good agreement with the theoretical curve. The upper (lower) bound of the curve of n_{cr} indicates the number of particles that can leave the system more quickly with Strategy SS (Strategy SW) than with Strategy SW (Strategy SS), even if N is large.

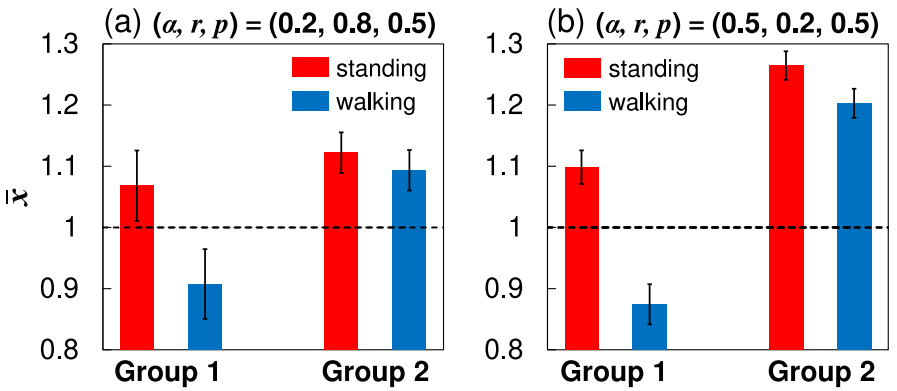

Fig. 16. Calculated values of $\bar{x}$ of standing- (red) and walking-preference (blue) particles for two groups with $(\alpha, r, p) \in \{(a)(0.2, 0.8, 0.5), (b)(0.5, 0.2, 0.5)\}$, with fixed $N = 1000$. The error bars represent one sample standard deviation for 1000 trials.

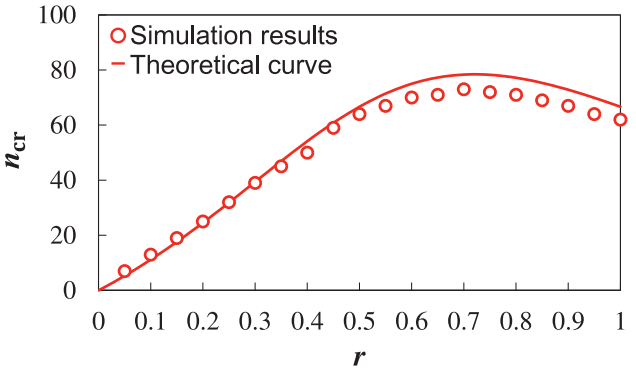

Fig. 17. Simulation (dots) and theoretical (curve) values of n_{cr} as a function of r. The other parameters are fixed as $\alpha = 0.5$ and $p = 0.5$. We note that the simulation values of n_{cr} satisfy $\tau_{SS}(n = n_{cr}) > \tau_{SW}(n = n_{cr})$ and $\tau_{SS}(n = n_{cr} + 1) < \tau_{SW}(n = n_{cr} + 1)$.

In addition, n_{cr} takes the maximal value around $r = 0.7$ in Fig. 17. If we notice the third term of τ_{SW} in Eq. (35) for $n > n_2$, the numerator is maximized when $r = 1$ (see also Eq. (34)), while the denominator is maximized when $r = 0.5$ (see Appendix A). The former (latter) corresponds to the positive effect of walking (the negative effect of preference). Therefore, for fixed (n, α, p), τ_{SW} takes its maximum value in the range $0.5 < r < 1$, which implies that n_{cr} also takes its maximal value in the range $0.5 < r < 1$.

6. Conclusion

We have analyzed three strategies for movement on an escalator: (i) two standing lanes (Strategy SS), (ii) one standing lane with one walking lane (Strategy SW), and (iii) two walking lanes (Strategy WW). These strategies were modeled with a modified two-lane TASEP. The specific contributions of this study are as follows.

In Section 3, we found that the one-lane model with our modified updating rules exhibits only the LD phase for all values of p, and that the steady-state flow for any p is identical to that of the original open-boundary TASEP with $p = 1$. This indicates that walking on an escalator does not affect steady-state flow, which is consistent with the results in [17].

In Section 4, we considered the total transportation time T for finite number of particles, using theoretical analyses and numerical simulations. In steady state, Q_{SS} is equal to Q_{WW} and is always greater than Q_{SW}. For example, Q_{SW} decreases at 33%–50% compared to Q_{SS} in the most-congested situations ($\alpha = 1$). This finding is consistent with the results of a pilot performed in the London underground in 2015 [8]; when 'standing only' was specified for escalators at Holborn station, about 30% more customers could use an escalator during the busiest times when both lanes were used only for standing.

Since $Q_{SS} = Q_{WW}$, counter-intuitively, $T_{SS} \approx T_{WW}$ for sufficiently large N, and T_{SS} is generally smaller than T_{SW}, indicating that Strategy SS is advantageous for large N. On the other hand, in limited cases for small N, Strategy SW can be more useful. Those differences arise because the negative effect of preference generally exceeds the positive effect of walking with Strategy SW for large N, while this relation is reversed for small N.

We have determined the reversal point $N = N_{cr}$ and $r = r_{cr}$, which satisfy $T_{SS}(N = N_{cr}) = T_{SW}(N = N_{cr})$ and $T_{SS}(r = r_{cr}) = T_{SW}(r = r_{cr})$. These values confirm that Strategy SW is advantageous mainly for small α, large r, large p, and small N.

In Section 5, we considered the individual transportation time τ using theoretical analyses and numerical simulations. Even if N is large, in which Strategy SS is advantageous in terms of reducing T, the first-leaving n_{cr} particles, mainly including walking-preference particles, can leave the system more quickly under Strategy SW than under Strategy SS. This behavior arises because the positive effect of walking is more active than the negative effect of preference in this case.

Applying the results of the present paper to real situations, we find that encouraging pedestrians to only stand on an escalator, which has recently been suggested by practitioners, is indeed beneficial for improving pedestrian flow, especially when a large number of pedestrians (large N) are using a facility. Conversely, providing a walking lane can improve pedestrian flow in limited cases in which the entrance is relatively uncongested (small α), the fraction of walking-preference pedestrians is high (large r), and the walking velocity is large (large p) with a small number of pedestrians (small N). In addition, the first-entering walking-preference pedestrians tend to benefit from Strategy SW.

More realistic models and comparisons with field data will be needed to more clearly relate our findings to the real world. For example, combining multiple models of escalators and floor fields, like a cellular-automaton pedestrian model [36], remains as a future work, along with fitting using actual data. Even so, the simple model discussed above offers useful insights as a first step.

Declaration of competing interest

The authors declare that they have no known competing financial interests or personal relationships that could have appeared to influence the work reported in this paper.

CRediT authorship contribution statement

Hiroki Yamamoto: Conceptualization, Data curation, Formal analysis, Investigation, Methodology, Software, Writing - original draft, Visualization. **Daichi Yanagisawa:** Funding acquisition, Supervision, Resources, Validation, Writing - review & editing. **Katsuhiro Nishinari:** Funding acquisition, Project administration, Resources, Writing - review & editing.

Acknowledgments

We greatly appreciate Airi Goto for her fruitful comments. This work was partially supported by JST-Mirai Program Grant Number JPMJMI17D4, Japan, JSPS KAKENHI Grant Number JP15K17583, and MEXT as 'Post-K Computer Exploratory Challenges' (Exploratory Challenge 2: Construction of Models for Interaction Among Multiple Socioeconomic Phenomena, Model Development and its Applications for Enabling Robust and Optimized Social Transportation Systems) (Project ID: hp180188).

Appendix A. Properties of Q_{SW}

In this appendix, we give the details of the properties of Q_{SW}, i.e., Eq. (6), as a function of α and r.

Defining $f(\alpha, r)$ as

$$Q_{\mathrm{SW}} = f(\alpha, r) = \frac{(1-r)\alpha}{1+(1-r)\alpha} + \frac{r\alpha}{1+r\alpha}, \tag{40}$$

$f(\alpha, r)$ can be rewritten as

$$f(\alpha, r) = 2 - \frac{1}{1+r\alpha} - \frac{1}{1+(1-r)\alpha}. \tag{41}$$

Therefore, for fixed r ($0 \le r \le 1$), $f(\alpha, r) = f(\alpha)$ is obviously a monotonically increasing function of α ($0 \le \alpha \le 1$). We assume that α is constant hereafter. Replacing $r\alpha$ with x for simplicity, $f(\alpha, r) = f(x)$ can be written as

$$f(x) = \frac{\alpha - x}{1+\alpha-x} + \frac{x}{1+x}, \tag{42}$$

where $0 \le x \le \alpha$. Taking the first derivation of $f(x)$, $df(x)/dx$ is calculated as

$$\frac{df(x)}{dx} = \frac{(\alpha - 2x)\{2+\alpha+4x(\alpha-x)\}}{(1+x)^2(1+\alpha-x)^2}. \tag{43}$$

The results of the first derivative test are summarized in Table 6. $f(x)$ takes its maximum value $2\alpha/(2+\alpha)$ with $x = \alpha/2$ ($r = 0.5$).

Therefore, $f(\alpha, r)$ takes its maximum value ($f(\alpha, r) = 2/3$) when $\alpha = 1$ and $r = 0.5$. Fig. 18 shows the calculated values of $f(\alpha, r)$ in the (α, r) plane. From Fig. 18, $f(\alpha, r)$ is sensitive to r for large α.

Table 6
Result of the first derivative test of $f(x)$.

x	0	...	$\frac{\alpha}{2}$	...	α
$f(x)$		↗	$f\left(\frac{\alpha}{2}\right)$	↘	
$\frac{df(x)}{dx}$	+	+	0	−	−

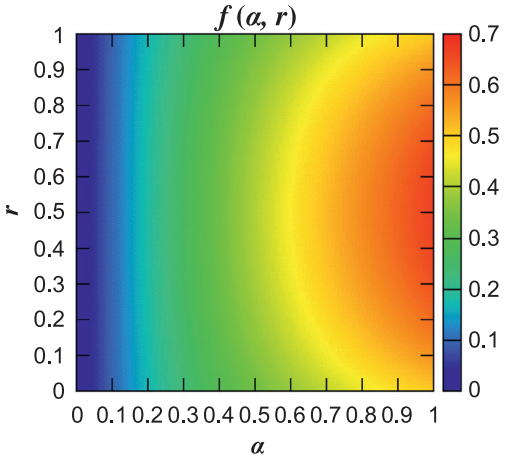

Fig. 18. Theoretical values of $f(\alpha, r)$ for various (α, r).

Appendix B. Revised escalator models

This appendix examines two revised escalator models: (1) walking-preference particles can enter both lanes (a standing lane and a walking lane) and change their lane to the walking lane in the bulk and (2) walking-preference particles can walk immediately after entering the walking lane.

B.1. Revised model 1

In Revised model 1, walking-preference particles enter the standing lane if the entrance of the walking lane is occupied and that of the standing lane is vacant. Then, they walk in the standing lane and change their lane if they catch up with their leading particles. When they change their lane, the walking-preference particles in the walking lane are prioritized. The details of the rule of changing lanes are summarized in Fig. 19.

Fig. 20 plots the simulation values of Q_{SW} with Revised model 1 (Q_{SW_R1}) for (a) $r = 0.5$ and (b) $r = 1$, comparing with the theoretical ones with the original updating rule.[3] We observe that Q_{SW_R1} is improved compared to Q_{SW} with the original rule (Q_{SW_o}); however, it is still less than Q_{SS} excluding an extreme case $r = 1$ (when $r = 1$, i.e., there are only walking-preference particles, Q_{SW} yields to Q_{SS}). This is mainly because standing-preference particles are still forced to wait in front of the entrance when more than two standing-preference particles consecutively attempt to enter the escalator. We note that changing lanes in the bulk does not suppress Q_{SW} because there are no jams in the walking lane due to the priority rule and walking-preference particles hop at the velocity no less than standing-preference particles.

We can also consider another possible updating rule, where standing- and walking-preference particles can enter either lane and they can change their lane in the bulk. However, the simulation is here abbreviated because (i) the flow clearly yields to Q_{SS} and (ii) it is not plausible that the standing pedestrians bother walking pedestrians in actual situations.

B.2. Revised model 2

In Revised model 2, walking-preference particles can walk immediately after entering the walking lane when the first site is vacant as in Table 7.

Fig. 21 plots the simulation values of Q_{SW} with Revised model 2 (Q_{SW_R2}) for (a) $r = 0.5$ and (b) $r = 1$, comparing with the theoretical ones with the original updating rule. We here observe two important phenomena. First, like Revised model 1, Q_{SW_R2} is improved compared to Q_{SW_o}; however, it is still less than Q_{SS}. This is mainly because standing-preference

[3] The theoretical values are plotted in this figure because the theoretical curves of Q_{SS}, Q_{WW}, and Q_{SW} with the original updating rule well agree with the simulation values.

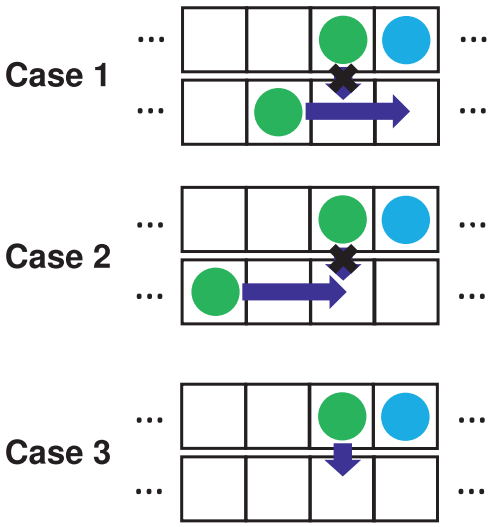

Fig. 19. Updating rules of changing lanes in Revised model 1 for walking-preference particles. The green particles prefer walking and the blue particles indifferently represent standing- or walking-preference particles. In each panel, the upper (lower) lane represents a standing (walking) lane. The walking-preference particles which entered the standing lane attempt to change their lane if they catch up with their leading particles. The walking-preference particles in the walking lane are prioritized; therefore, the walking-preference particles in the standing lane can change their lane only in Case 3. We note that in Case 2 the walking-preference particle may hop only one site; however, changing lanes is prohibited for simplicity.

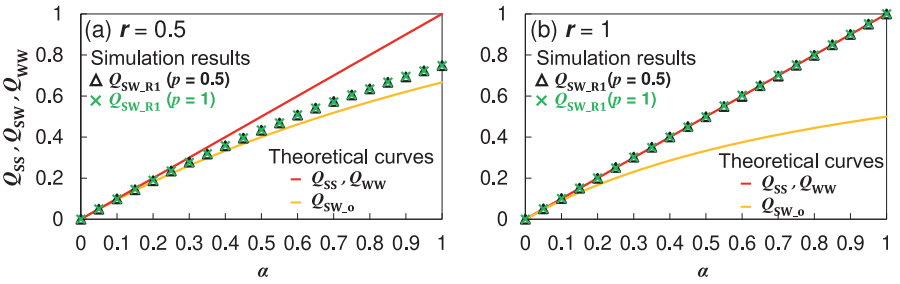

Fig. 20. Simulation values (dots) of Q_{SW_R1} for (a) $r = 0.5$ and (b) $r = 1$ with $p \in \{0.5$(black triangles), 1(green crosses)$\}$ as functions of α, comparing with the theoretical values (red/orange curves) values of Q_{SS}, Q_{WW}, and Q_{SW_o}.

Table 7
Updating rules of the left boundary in Revised model 2 for walking-preference particles. In this model, walking-preference particles can immediately walk after entering the walking lane if the first site is vacant. We note that this figure describes the case of $p = 1$.

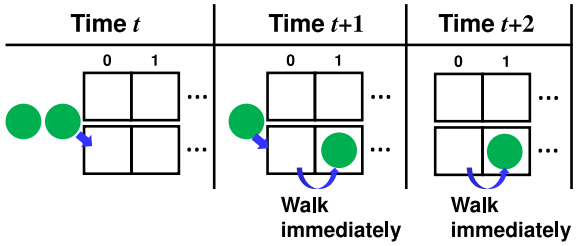

particles are forced to wait in front of the entrance when more than two standing-preference particles consecutively attempt to enter the system. Second, the more p approaches to 1, the more Q_{SW} is improved because the possibility that the first site is vacant becomes higher with larger p.

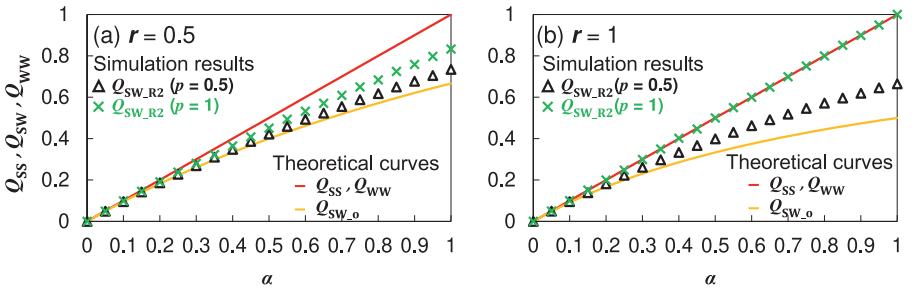

Fig. 21. Simulation values (dots) of Q_{SW_R2} for (a) $r = 0.5$ and (b) $r = 1$ with $p \in \{0.5$(black triangles), 1(green crosses)$\}$ as functions of α, comparing with the theoretical values (red/orange curves) values of Q_{SS}, Q_{WW}, and Q_{SW_o}.

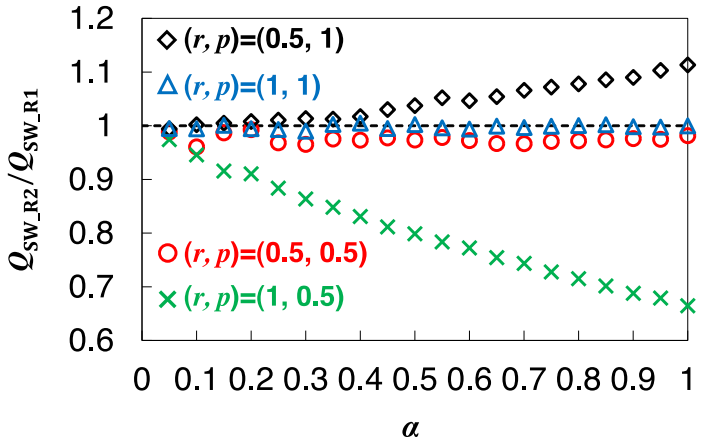

Fig. 22. Calculated values of the ratios Q_{SW_R2}/Q_{SW_R1} as functions of α for various $(r, p) \in \{(0.5, 1)$(black diamonds), $(1, 1)$(blue triangles), $(0.5, 0.5)$(red circles), $(1, 0.5)$(green crosses)$\}$.

B.3. Comparison of revised model 1 and 2

We here stress that Q_{SW_R1} is generally equal or larger than Q_{SW_R2} for $p = 0.5$, whereas vice versa for $p = 1$, as shown in Fig. 22. These phenomena can be explained mainly as follows: in Revised model 1, a standing-preference particle just after two consecutive walking-preference particles cannot enter the standing lane, while two consecutive walking-preference particles can always enter the system. On the other hand, in Revised model 2, a standing-preference particle just after two consecutive walking-preference particles can always enter the standing lane, while two consecutive walking-preference particles sometimes cannot enter the system when $p < 1$. These conflicting effects cause the reverse of the inequality relation between Q_{SW_R1} and Q_{SW_R2} dependent on p. We note that Q_{SW_R2}/Q_{SW_R1} yields to 1 with $(r, p) = (1, 1)$ because there are only walking-preference particles and they can always enter the system in the both models.

Appendix C. Detailed calculations of T_{SW}

In this appendix, we discuss the detailed calculations for obtaining the general form of T_{SW}.

The specific calculations are summarized as Eq. (44). We note that the third term of the fourth line in Eq. (44) is the summation of an arithmetic–geometric sequence, and therefore, we can obtain a closed-form expression.

$$
\begin{aligned}
T_{SW} &\approx \sum_{k=1}^{N+1} P(k) t_{SW}(k) \\
&= \frac{1}{\alpha} + \sum_{k=1}^{N_1} \{P(k)(T_{SW}^{s}(N-k+1) + T_{S}^{f})\} + \left(1 - \sum_{k=1}^{N_1} P(k)\right)(T_{SW}^{s}(N) + T_{W}^{f}) \\
&= \frac{1}{\alpha} + \sum_{k=1}^{N_1} \left\{(1-r)r^{k-1}\left(\frac{N-k}{Q_{SW}} + \frac{L}{1}\right)\right\} + \left(1 - \sum_{k=1}^{N_1}(1-r)r^{k-1}\right)\left(\frac{N-1}{Q_{SW}} + \frac{L}{1+p}\right)
\end{aligned}
$$

$$
\begin{aligned}
&= \frac{1}{\alpha} + \frac{N-1}{Q_{\mathrm{SW}}} - \sum_{k=1}^{N_1} \frac{(k-1)(1-r)r^{k-1}}{Q_{\mathrm{SW}}} + \frac{(1-r^{N_1})L}{1} + \frac{r^{N_1}L}{1+p} \\
&= \begin{cases} \dfrac{1}{\alpha} + \dfrac{N-1}{\frac{r\alpha}{1+r\alpha} + \frac{(1-r)\alpha}{1+(1-r)\alpha}} - \dfrac{\frac{r}{1-r}\{1 - N_1 r^{N_1-1} + (N_1-1)r^{N_1}\}}{\frac{r\alpha}{1+r\alpha} + \frac{(1-r)\alpha}{1+(1-r)\alpha}} + \dfrac{(1-r^{N_1})L}{1} + \dfrac{r^{N_1}L}{1+p} & \text{for } r \neq 1 \\ \dfrac{1}{\alpha} + \dfrac{N-1}{\frac{\alpha}{1+\alpha}} + \dfrac{L}{1+p} & \text{for } r = 1 \end{cases} \\
&= \frac{1}{\alpha} + \frac{N-1}{\frac{r\alpha}{1+r\alpha} + \frac{(1-r)\alpha}{1+(1-r)\alpha}} - \frac{\sum_{k=1}^{N_1}(1 - r^{N_1-k})r^k}{\frac{r\alpha}{1+r\alpha} + \frac{(1-r)\alpha}{1+(1-r)\alpha}} + \frac{(1-r^{N_1})L}{1} + \frac{r^{N_1}L}{1+p}
\end{aligned} \tag{44}
$$

Appendix D. Discussion of the behavior of $T_{\mathrm{SW}} - T_{\mathrm{SS}}$ when $\alpha_1 < \alpha \leq 1$ for sufficiently large N

In this appendix, we discuss the behavior of $T_{\mathrm{SW}} - T_{\mathrm{SS}}$ when $\alpha_1 < \alpha \leq 1$ for sufficiently large N.

For sufficiently large N; especially $N \gg N_0$, $N_1 = N_0$, due to $N_1 = \min(N_0, N)$. Therefore, using Eq. (18), $T_{\mathrm{SW}} - T_{\mathrm{SS}}$ can be represented as follows:

$$
\begin{aligned}
&T_{\mathrm{SW}} - T_{\mathrm{SS}} \\
&= (N-1)\left(\frac{1}{Q_{\mathrm{SW}}} - \frac{1}{Q_{\mathrm{SS}}}\right) - \frac{\sum_{k=1}^{N_0}(1 - r^{N_0-k})r^k}{Q_{\mathrm{SW}}} - \frac{pr^{N_0}}{1+p}\frac{L}{1} \\
&= \frac{1}{Q_{\mathrm{SW}}}\left\{(N-1)\left(1 - \frac{1-r}{1+(1-r)\alpha} - \frac{r}{1+r\alpha}\right) - \sum_{k=1}^{N_0}(1 - r^{N_0-k})r^k - \frac{pr^{N_0}L}{1+p}\left(2 - \frac{1}{1+r\alpha} - \frac{1}{1+(1-r)\alpha}\right)\right\} \\
&= \frac{1}{Q_{\mathrm{SW}}}\left\{N - 1 - \frac{A}{1+(1-r)\alpha} - \frac{B}{1+r\alpha} - C\right\} \\
&= \frac{g(\alpha)}{Q_{\mathrm{SW}}},
\end{aligned} \tag{45}
$$

where A, B, and C can be regarded as constant values; specifically,

$$
A = (1-r)(N-1) + \frac{pr^{N_0}L}{1+p} > 0, \tag{46}
$$

$$
B = r(N-1) + \frac{pr^{N_0}L}{1+p} > 0, \tag{47}
$$

$$
C = \sum_{k=1}^{N_0}(1 - r^{N_0-k})r^k + \frac{2pr^{N_0}L}{1+p} > 0. \tag{48}
$$

and

$$
g(\alpha) = N - 1 - \frac{A}{1+(1-r)\alpha} - \frac{B}{1+r\alpha} - C. \tag{49}
$$

$dg(\alpha)/d\alpha$ can be calculated as

$$
\frac{dg(\alpha)}{d\alpha} = \frac{(1-r)A}{\{1+(1-r)\alpha\}^2} + \frac{rB}{(1+r\alpha)^2} > 0. \tag{50}
$$

Therefore, for sufficiently large N, $g(\alpha)$ is a monotonically increasing function when $\alpha_1 < \alpha \leq 1$. Considering this fact together with $g(\alpha_1) > 0$ for sufficiently large N, $g(\alpha) > 0$, and therefore,

$$
T_{\mathrm{SW}} - T_{\mathrm{SS}} > 0, \tag{51}
$$

when $\alpha_1 < \alpha \leq 1$.

Appendix E. Discussion of the behavior of $h(\alpha)$ when $0 < \alpha \leq \alpha_1$ for sufficiently large N

Here, we discuss the details of the behavior of $h(\alpha)$ when $0 < \alpha \leq \alpha_1$ for sufficiently large N. The function $h(\alpha)$ can be rewritten as follows:

$$
h(\alpha) = 1 - \frac{1-r}{1+(1-r)\alpha} - \frac{r}{1+r\alpha} - \frac{rpL}{(1+p)(N-1)}\left\{\frac{(1-r)\alpha}{1+(1-r)\alpha} + \frac{r\alpha}{1+r\alpha}\right\}
$$

$$= 1 - \frac{2rpL}{(1+p)(N-1)} - \frac{1 - r - \frac{rpL}{(1+p)(N-1)}}{1+(1-r)\alpha} - \frac{r - \frac{rpL}{(1+p)(N-1)}}{1+r\alpha}$$
$$= 1 - \frac{2rpL}{(1+p)(N-1)} - \frac{D}{1+(1-r)\alpha} - \frac{E}{1+r\alpha}, \tag{52}$$

where D and E are represented as

$$D = 1 - r - \frac{rpL}{(1+p)(N-1)} \tag{53}$$

and

$$E = r - \frac{rpL}{(1+p)(N-1)}. \tag{54}$$

For sufficiently large N, which especially satisfies $D > 0$ and $E > 0$; specifically,

$$N > \frac{pL}{1+p} \max\left(\frac{r}{1-r}, 1\right) + 1, \tag{55}$$

$dh(\alpha)/d\alpha$ can be calculated as

$$\frac{dh(\alpha)}{d\alpha} = \frac{(1-r)D}{\{1+(1-r)\alpha\}^2} + \frac{rE}{(1+r\alpha)^2} > 0. \tag{56}$$

Therefore, for sufficiently large N, $h(\alpha)$ is a monotonically increasing function when $0 < \alpha \leq \alpha_1$. Considering this fact together with $h(0) = 0$, $h(\alpha) > 0$, and therefore,

$$T_{SW} - T_{SS} > 0, \tag{57}$$

when $0 < \alpha \leq \alpha_1$.

References

[1] T. Elevator, Am. Nat. Stand. Saf. Code Am. Soc. Mech. Eng. ANSI A 17 (1971).
[2] G.R. Strakosch, The Vertical Transportation Handbook, John Wiley & Sons, 1998.
[3] M. Mason, Walk the Lines: The London Underground, Overground, Random House, 2011.
[4] M. Toda, S. Takahashi, 2018 IEEE International Conference on Systems, Man, and Cybernetics (SMC), IEEE, 2018, pp. 1156–1161.
[5] M. Toki, Bull. Edogawa Univ. 25 (2015) (in Japanese).
[6] Escalator Etiquette: The Dos and Don'ts, BBC News, 2013, (accessed February 22, 2019), https://www.bbc.com/news/magazine-23444086.
[7] Keep it to the Left, THE AGE, 2005, (accessed February 22, 2019), https://www.theage.com.au/national/keep-it-to-the-left-20050729-ge0lhc.html.
[8] C.H.N. Kukadia, P. Stoneman, G. Dyer, NECTAR 11 (2016).
[9] Campaign on Non-Walking in Escalators in Tokyo Station (in Japanese), JR East, 2018, (accessed February 22, 2019), https://www.jreast.co.jp/press/2017/tokyo/20181211_t01.pdf.
[10] Why You Shouldn't Walk on Escalators, The New York Times, 2017, (accessed February 22, 2019), https://www.nytimes.com/2017/04/04/us/escalators-standing-or-walking.html.
[11] P. Kauffmann, Ph.D. thesis, Virginia Tech. 2011.
[12] W. Li, J. Gong, P. Yu, S. Shen, R. Li, Q. Duan, Physica A 420 (2015) 28.
[13] F. Al Widyan, A. Al-Ani, N. Kirchner, M. Zeibots, Australasian Transport Research Forum, ATRF, 2016.
[14] C. Cheung, W.H. Lam, J. Traffic Transp. 124 (1998) 277.
[15] X. Ji, J. Zhang, B. Ran, Physica A 392 (2013) 5089.
[16] P. Kauffmann, S. Kikuchi, Transp. Res. Rec. 136 (2013).
[17] F.-R. Yue, J. Chen, J. Ma, W.-G. Song, S.-M. Lo, Chin. Phys. B 27 (2018) 124501.
[18] A. Parmeggiani, T. Franosch, E. Frey, Phys. Rev. Lett. 90 (2003) 086601.
[19] D. Chowdhury, A. Schadschneider, K. Nishinari, Phys. Life Rev. 2 (2005) 318.
[20] T. Chou, K. Mallick, R. Zia, Rep. Progr. Phys. 74 (2011) 116601.
[21] C. Appert-Rolland, M. Ebbinghaus, L. Santen, Phys. Rep. 593 (2015) 1.
[22] D. Helbing, Rev. Modern Phys. 73 (2001) 1067.
[23] T. Imai, K. Nishinari, Phys. Rev. E 91 (2015) 062818.
[24] H. Ito, K. Nishinari, Phys. Rev. E 89 (2014) 042813.
[25] H. Yamamoto, D. Yanagisawa, K. Nishinari, J. Stat. Mech. 2017 (2017) 043204.
[26] D. Yanagisawa, A. Tomoeda, R. Jiang, K. Nishinari, JSIAM Lett. 2 (2010) 61.
[27] C. Arita, D. Yanagisawa, J. Stat. Phys. 141 (2010) 829.
[28] C. Arita, A. Schadschneider, Math. Models Methods 25 (2015) 401.
[29] J. de Gier, B. Nienhuis, Phys. Rev. E 59 (1999) 4899.
[30] R.A. Blythe, M.R. Evans, J. Phys. A 40 (2007) R333.
[31] B. Derrida, M.R. Evans, V. Hakim, V. Pasquier, J. Phys. A 26 (1993) 1493.
[32] M. Evans, Y. Kafri, K. Sugden, J. Tailleur, J. Stat. Mech. 2011 (2011) P06009.
[33] Y.-Q. Wang, R. Jiang, Q.-S. Wu, H.-Y. Wu, Modern Phys. Lett. B 28 (2014) 1450123.
[34] H. Hilhorst, C. Appert-Rolland, J. Stat. Mech. 2012 (2012) P06009.
[35] T. Reichenbach, E. Frey, T. Franosch, New J. Phys. 9 (2007) 159.
[36] C. Burstedde, K. Klauck, A. Schadschneider, J. Zittartz, Physica A 295 (2001) 507.